DESIGN OF THERMOSYPHON SOLAR DOMESTIC HOT WATER SYSTEMS

by

MARK P. MALKIN

A thesis submitted in partial fulfillment of the
requirements for the degree of

MASTER OF SCIENCE

(Mechanical Engineering)

at the

UNIVERSITY OF WISCONSIN-MADISON

1985

DESIGN OF THERMOSYPHON SOLAR DOMESTIC HOT WATER SYSTEMS

by Mark P. Malkin

Under the Supervision of Professor Sanford A. Klein

Thermosyphon solar domestic hot water heating systems operate at low, self regulated collector flow rates. Their performance is generally better than active (i.e., pumped) systems operating at conventional flow rates, and is comparable to pumped systems operating at low collector flow rates. A study of thermosyphon systems has been undertaken to determine collector flow rates and thermal stratification in storage tanks, assess how these flow rates relate to those used in pumped systems with various control strategies, and develop a design method for thermosyphon systems based on equivalent flow rates for pumped systems. The design method for estimating long term performance is based on the original f-Chart method, and requires only monthly average meteorological data and a description of the system component geometry as inputs. Thermal stratification in the storage tank is accounted for through use of a modified collector heat loss coefficient. The varying flow rate throughout the day and year in a thermosyphon system is accounted for through use of a fixed monthly "equivalent average" flow rate. The "equivalent average" flow rate is that which balances the thermosyphon buoyancy driving force with the frictional losses in the flow circuit on a monthly average basis. Comparison between the annual solar fraction pre-

dicted by the design method and TRNSYS simulations for a wide range of thermosyphon solar DHW systems shows an RMS error of 2.6%.

APPROVED:

12/4/85
Date

S. A. Klein
Sanford A. Klein, Professor
Mechanical Engineering

ACKNOWLEDGEMENTS

I would like to thank my thesis advisors, Professors Jack Duffie and Sandy Klein, for their guidance and encouragement throughout this project. Thanks also to Jim Braun for his computer help, and to my friends in the Solar Lab for making the Lab much more than just a place to work. Lastly, a special thank you to a special person, Linda (alias Jack), for her caring and confidence.

Financial support for this work was provided by a grant from the U.S. Department of Energy.

TABLE OF CONTENTS

LIST OF FIGURES

LIST OF TABLES

NOMENCLATURE

A	coefficient for Evans' utilizability correlation
A_c	collector area
A_i	surface area of tank - collector inlet connecting pipe
A_o	surface area of collector outlet - tank connecting pipe
A_s	cross sectional area of storage tank
B	coefficient for Evans' utilizability correlation
C_1	coefficient for Copsey's correlation
C_2	coefficient for Copsey's correlation
C_3	coefficient for Copsey's correlation
C_4	coefficient for Copsey's correlation
C_p	collector fluid specific heat
C_{ps}	storage water specific heat
d	diameter of collector risers, headers, or connecting pipe
d_1	inlet diameter
d_2	outlet diameter
E	collector effectiveness
f	Darcy friction factor
F	solar fraction
F'	collector efficiency factor
F_R	collector heat removal factor
g	acceleration due to gravity

h_F	friction head loss
h_T	thermosyphon buoyancy driving force
H	height of storage tank
H_1	height of collector inlet above reference
H_2	height of collector outlet above reference
H_3	height of connecting pipe inlet to storage above reference
H_5	height of tank return to collector above reference
H_6	height of top of storage tank above reference
H_T	daily solar radiation incident on the collector
I	hourly solar radiation incident on the horizontal
I_b	hourly beam solar radiation on the horizontal
I_c	critical radiation level
I_d	hourly diffuse solar radiation on the horizontal
I_T	hourly solar radiation incident on the collector
I_0	hourly extraterrestrial radiation
k	right angle bends in connecting pipe
K	thermal conductivity of water in storage tank
K_s	stratification coefficient
K_T	clearness index
K_T'	modified clearness index for Evans' correlation
l	length of collector risers, headers, or connecting pipe
L	monthly hot water heating load
$\dot{m}$	collector fluid flow rate

$\dot{m}_L$	hot water load flow rate
$\dot{m}_{test}$	collector fluid flow rate during ASHRAE 93-77 test
M	mixing number
$\overline{M}_c/M_L$	ratio of daily collector flow to load flow
N	units correction
N_k	number of collector nodes
N_p	collector pump operating time
Q_{aux}	auxiliary energy requirement
Q_{loss}	storage tank heat loss
Q_{sup}	energy supplied to load
Q_u	useful solar energy gain
Q_u-P	useful solar energy gain including connecting pipe heat loss
Re	Reynolds' number
S	absorbed solar radiation
S_i	specific gravity of collector fluid at collector inlet
S_o	specific gravity of collector fluid at collector outlet
T	temperature (°C)
T_a	ambient temperature
T_{ave}, T_{tank}	average temperature of water in storage tank
T_i, T_{ret}	collector fluid inlet temperature
T_k	temperature at the midpoint of a collector node
T_{mains}	mains water temperature
T_o, T_{out}	collector fluid outlet temperature

T_{pi}	pipe inlet temperature
T_{po}	pipe outlet temperature
T_{set}	auxiliary heating water set temperature
T_{sol}	temperature of water from tank supplied to mixing valve
T_{sup}	temperature of water from mixing valve supplied to load
u	fluid velocity in connecting pipes
u_h	fluid velocity in collector headers
u_r	fluid velocity in collector risers
U_L	overall collector heat loss coefficient
U_p	thermal loss coefficient of the connecting pipe
UA	overall storage tank heat loss coefficient
$(UA)_p$	overall pipe heat loss coefficient
X	f-Chart correlation parameter
X_{mix}	f-Chart correlation parameter for fully mixed storage
X_{str}	f-Chart correlation parameter for stratified storage
Y	f-Chart correlation parameter
Y_{max}	f-Chart correlation parameter for $F_R = 1.$
Y_{mix}	f-Chart correlation parameter for fully mixed storage
Y_{str}	f-Chart correlation parameter for stratified storage
β	collector tilt angle (slope)
γ	collector azimuth angle
ϕ	latitude
Φ	utilizability
δ	declination angle

Δt	units correction
$\Delta X/\Delta X_{max}$	correction for stratified storage
ϵ	heat exchanger effectiveness
μ	fluid dynamic viscosity
$(\tau\alpha)$	transmittance - absorptance product
ω	hour angle

An overbar ($\bar{}$) indicates monthly average values.

CHAPTER 1: INTRODUCTION

Thermosyphon solar domestic hot water (DHW) systems are widely used in Australia and Israel, and are gaining popularity in Japan, the United States, and elsewhere. The collector fluid in a thermosyphon system is circulated by natural convection, eliminating the need for the pump and controller of an active (i.e., pumped) system.

The key to the operation of a thermosyphon system is the location of the storage tank above the collector. By piping the outlet of the collector to the top part of the storage tank, and the bottom of the storage tank to the collector inlet, a closed loop system is formed. During daylight hours, the collector fluid is heated and becomes warmer and less dense than the fluid in the storage tank. In a direct natural circulation system, water will flow through the collector risers and connecting piping, into the storage tank. Hot water may be drawn from the top of the tank to load, while colder mains water replenishes the bottom of the storage tank. A check valve may be included in the connecting piping to prevent reverse flow at night, when the water in the collector is at a lower temperature than the water in storage. The flow rate in a natural circulation thermosyphon system varies throughout the day and year, depending on the absorbed radiation, fluid temperatures, system geometry, and other factors. Thermosyphon systems may be described as self-adjusting, with increasing solar radiation leading to increasing flow rates through the collector [1].

A sketch of a thermosyphon system is shown in Fig. 1.1, illustrating the basic parts of a flat plate solar collector. The absorber plate is used to convert solar radiation to heat, which is then transferred to a fluid (water) that flows through the risers. The absorber plate and risers are usually coated black to enhance the energy absorption. Glass covers, usually single or double, are transparent to incoming solar radiation and relatively opaque to outgoing long wave radiation, creating a "greenhouse" effect. Glazings also protect the absorber plate from the environment and reduce convection heat loss. Insulation is applied to the back and edges of the absorber plate to reduce conduction heat loss.

Thermosyphon systems have some practical advantages and disadvantages compared with active solar DHW systems. A typical active system requires a pump to force the fluid to circulate through the collector. A differential temperature controller, sensing the temperatures at the bottom of the storage tank and at the outlet of the collector, turns the pump on and off, depending on the controller deadband settings. The pump has an inherent parasitic power requirement, albeit usually slight, and possible maintenance requirements. Furthermore, a malfunction of the controller, which is difficult to detect, can drastically lower the performance of an active solar heating system. Thermosyphon systems have no need for a pump or controller, and therefore avoid any problems which may be associated with their operation.

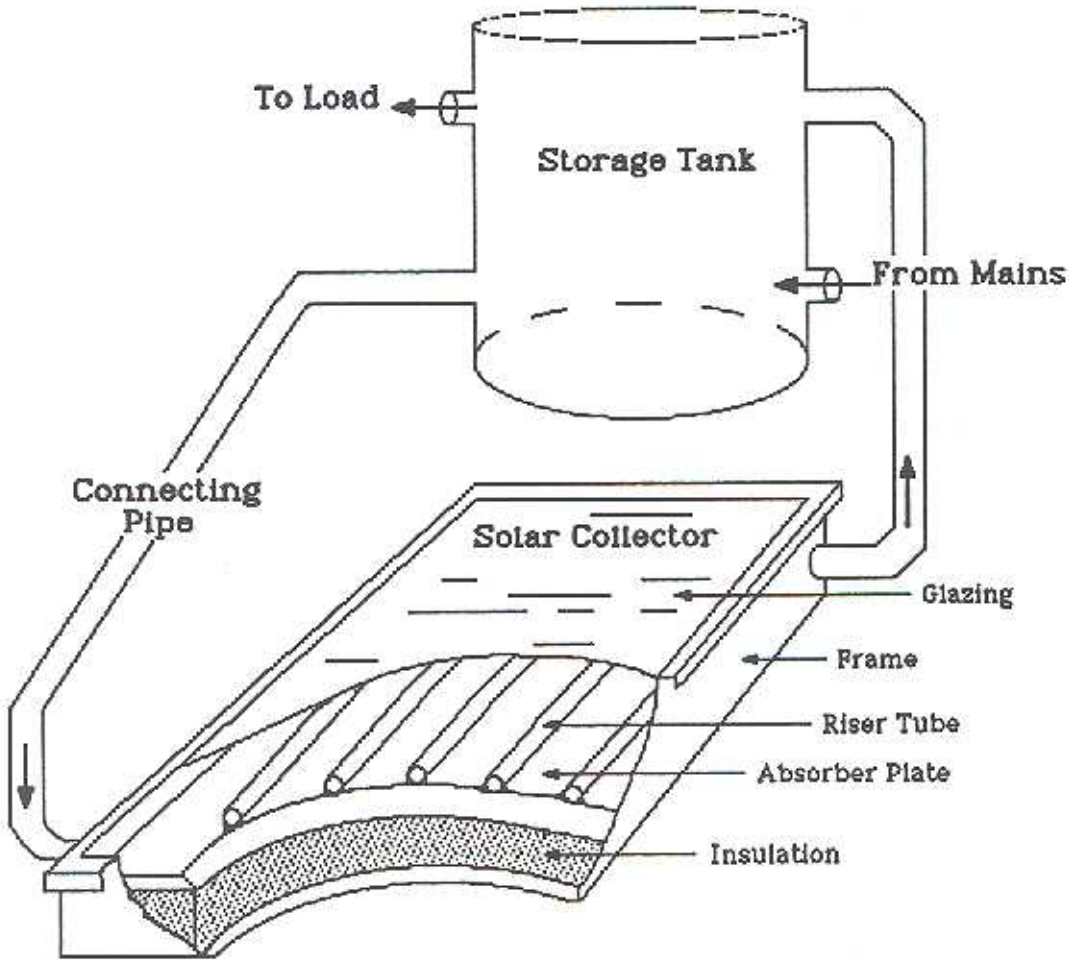

Figure 1.1 Thermosyphon system showing flat plate collector cross section

Several disadvantages of thermosyphon systems result from the need for locating the storage tank above the collector. For most residential uses, the collector array is mounted on the roof, and therefore the storage tank must also be mounted on the roof. In retrofit applications, the roof construction may not be adequately designed to handle the weight of a water storage tank. Besides structural problems, the location of the thermosyphon system storage tank outside, instead of in the basement as in most active systems, presents a thermal disadvantage. In an active system, heat loss from the storage tank in the winter may be considered as heat gain in aiding to meet the house's space heating requirement, while thermal loss to the environment in a thermosyphon system cannot be utilized. Careful consideration must be given to the insulation of the storage tank to minimize thermal losses. Lastly, a storage tank elevated on stilts on the roof of a house may pose aesthetic problems. A solution to this problem may be found by concealing the tank from view by a false chimney, or some other means of architectural integration in a new construction [2]. The aesthetic problems may be minimized by the "close coupled" thermosyphon system design, in which the storage tank is situated horizontally, directly above the collector. The "close coupled" design also has the advantage that the collector-piping-tank system is usually manufactured and marketed as a single unit, reducing plumbing costs.

1.1 Freeze Protection

In its basic form, a direct circulation thermosyphon solar DHW system is not suited to year round use in freezing climates, since water remains in the collector at all times. In areas where freezing is infrequent, freeze protection may be accomplished by installing auxiliary heaters in the lower headers of the collector panels [3]. An alternate method of freeze protection involves the use of manual or solenoid actuated automatic valves, to drain the water from the collector and connecting piping during freezing conditions. Strategies for freeze protection in a thermosyphon system are similar to those in a direct circulation active solar DHW system in which potable water is both the circulating and storage fluid. An active system however, is more easily configured for indirect circulation in which an antifreeze solution is circulated through the closed collector loop, and heat is transferred through a heat exchanger to the potable water for storage. Antifreeze systems, although more complicated than direct circulation systems, are more appropriate for year round use in very cold northern climates. Indirect circulation thermosyphon DHW systems are currently on the market, but are not considered in this study. A typical residential hot water heating load is equal, if not greater, in the summer than in the winter. Therefore, thermosyphon systems with direct circulation may be economically competitive with other systems, in all but the most severe climates, even if used only during the warmer spring, summer and fall months.

1.2 NBS Side by Side Test

The thermal performance of five liquid based solar DHW systems has been carefully monitored by the National Bureau of Standards (NBS) in Gaithersburg, Maryland [4]. All the systems were run side by side under identical meteorological conditions and each provided approximately 265 liters of hot water per day. The system configurations include a single tank direct circulation thermosyphon system (STDT), a single tank direct active system (STDA), a double tank direct active system (DTDA), a single tank indirect circulation active system with a wrap around heat exchanger (STIA), and a double tank indirect active system with a coil in tank heat exchanger (DTIA). All of the components of the direct circulation systems, with the exception of the storage tanks, are identical. A.H. Fanney and S.A. Klein [4] present a description of each of the five liquid based systems, plus one evacuated tube air system, and the instrumentation used to monitor their performance. Measurements of the collector performance characteristics, storage tank heat loss coefficients, heat exchanger effectiveness values for the two indirect systems, and storage tank temperature profiles are included. Schematic diagrams of the five liquid based systems appear in Figs. 1.2-1.6.

The fractional energy savings, by solar, for each of the systems during the one year time interval from January-December 1980 is shown graphically in Fig. 1.7. Parasitic energy use includes the energy requirement of the solenoid actuated freeze protection valves, and

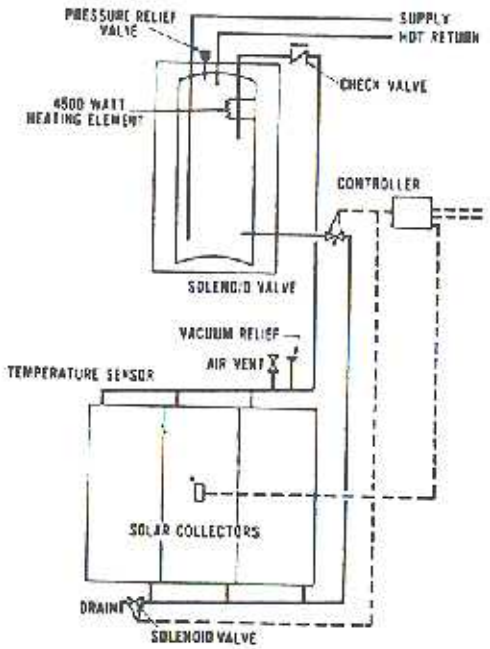

Figure 1.2 NBS single tank direct circulation thermosyphon system (STDT). From A.H. Fanney and S.A. Klein [4]

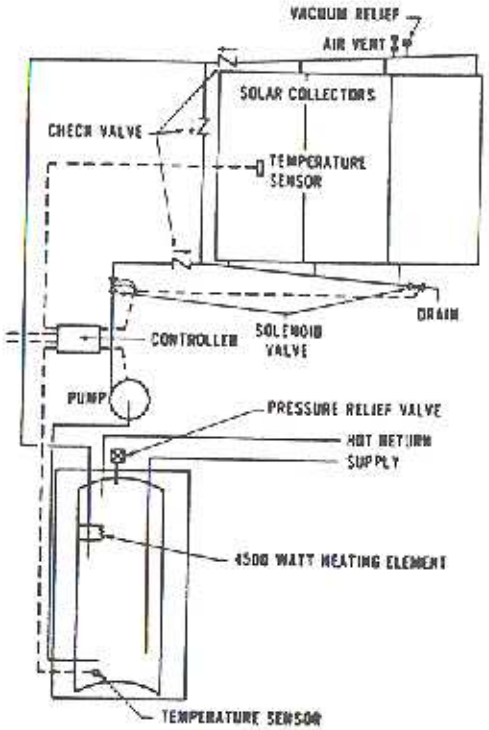

Figure 1.3 NBS single tank direct circ. active system (STDA). From [4]

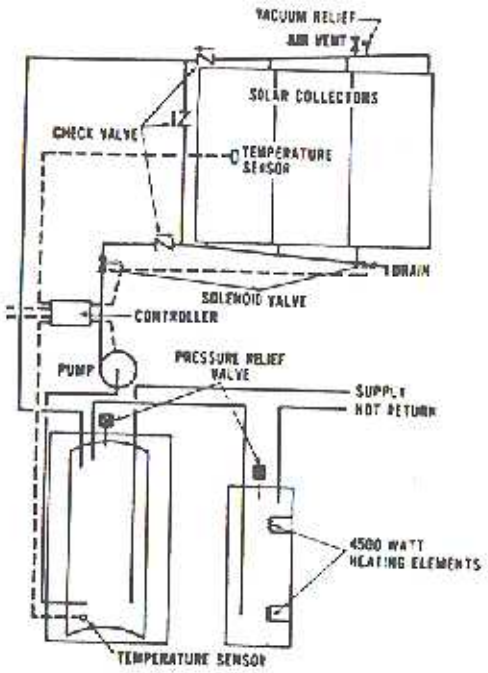

Figure 1.4 NBS double tank direct circ. active system (DTDA). From [4]

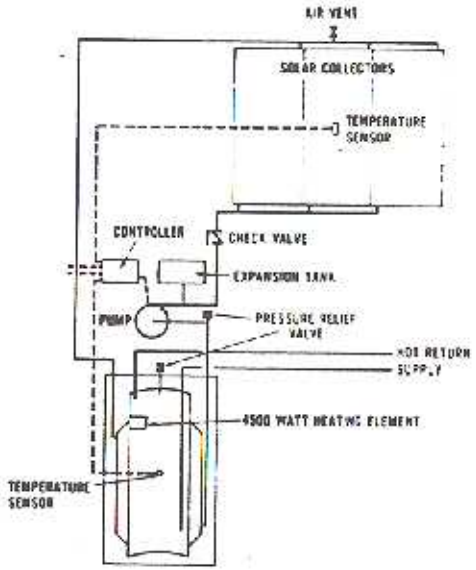

Figure 1.5 NBS single tank indirect circ. active system (STIA). From [4]

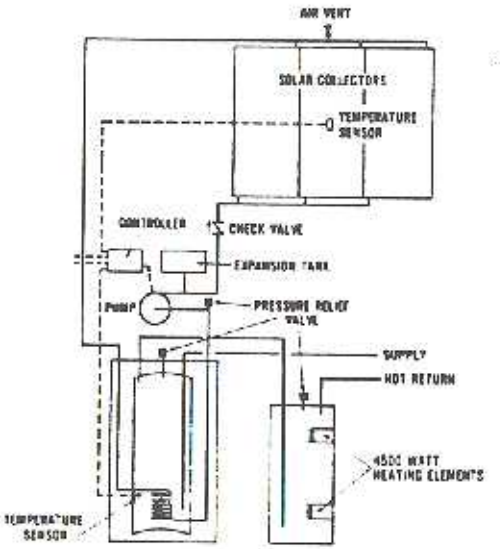

Figure 1.6 NBS double tank indirect circ. active system (DTIA). From [4]

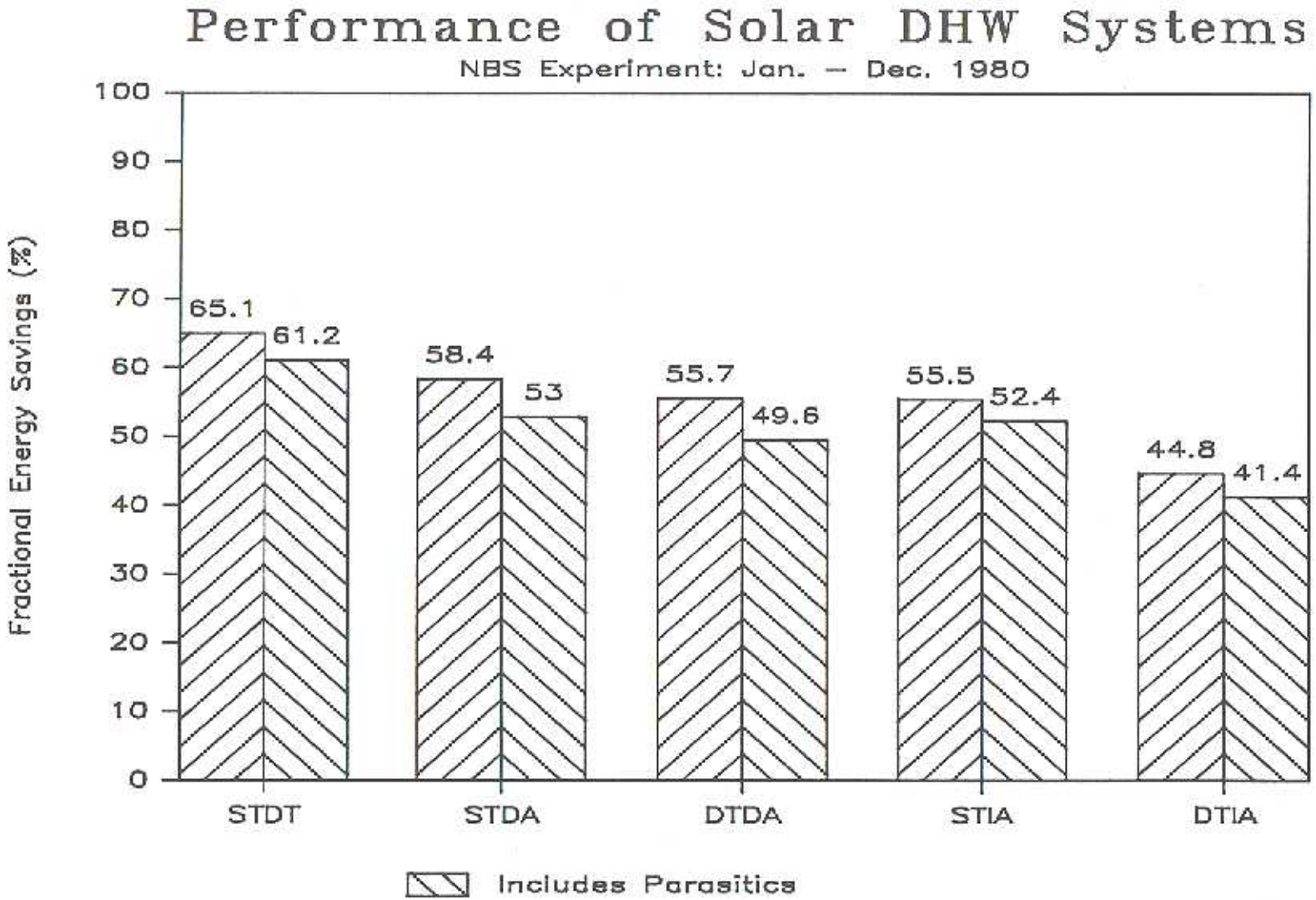

Figure 1.7 Annual fractional energy savings for five systems tested at NBS

the pump and controller of the active systems. Parasitic energy use results in a reduction of the fractional energy savings from between 3 and 6 percent, depending on the system. The effect of parasitic energy use on the solar fraction is greater for the direct systems as compared to the indirect systems because the fail safe freeze protection scheme used in the direct systems requires two solenoid valves to be energized continuously during non-freezing conditions. The direct circulation active systems require more parasitic power than the thermosyphon system due to their pump and controller.

The thermosyphon system requires the least amount of auxiliary energy of the six systems tested, and thus provides the greatest fractional energy savings by solar. The single tank direct circulation active system performs slightly better than the double tank system, which is consistent with earlier studies at NBS [5]. The smaller surface area in the single tank system results in less tank thermal energy loss than in the double tank system. However, the double tank system has a greater capacity to meet the heating loads during periods of insufficient solar radiation. A thermal performance comparison between single tank and double tank indirect systems cannot be made based on the side by side test, since different heat exchangers were used. A previous study at NBS in which identical heat exchangers were used, showed a single tank indirect system out performing a double tank indirect circulation system [5].

Three explanations may be given to account for the excellent relative performance of the thermosyphon system. First, the thermo-

syphon system tested is a single tank system and thus has lower thermal energy losses from the storage tank than the two tank systems. The storage tank volume of the thermosyphon system was the smallest of the five liquid systems. Second, the thermosyphon system is a direct system, and as a result it avoids the thermal penalty associated with heat exchange between the collector fluid and the stored water inherent to an indirect system. Third, and most important, the low flow rate through the thermosyphon collector array (measured to be less than 13 liters/hr-m^2) results in a high degree of thermal stratification in the storage tank. The low flow causes very little mixing of the water heated by the electric auxiliary heating element in the top of the tank with the fluid returning to the collector from the bottom of the tank. The lower return temperature from a stratified storage tank increases the collection efficiency by reducing thermal losses from the collector. This is seen from the Hottel-Whillier collector equation [1] where T_i is the temperature of fluid returned from the tank to the collector:

$$Q_u = A_c F_R [S - U_L (T_i - T_a)] \qquad (1.1)$$

The active systems were all operated with a pump set to force circulation through the collector array at 71 liters/hr-m^2. This high flow rate, on the order of five to six times the average flow rate through the thermosyphon system, causes the thermal stratification to be destroyed in the storage tank of the active systems.

The return fluid temperature is at a higher temperature than in the thermosyphon system, and thus greater thermal losses from the back and sides of the collector occur in the active systems. Recent experiments and simulations have shown that improved performance for active systems may be achieved with a flow rate on the order of 1/5 of the normal high rates used in most active systems [6,7]. It is probable that the performance of the direct circulation active systems could be enhanced by a low flow pump control strategy.

Based on the NBS side by side tests, it should not be concluded that a thermosyphon system will out perform an active system. The performance of a system depends a great deal on the configuration of the components, and the particular control strategy employed. However, it may be stated that the performance of a well designed thermosyphon system can be comparable to that of a well designed active system, and that due to its low maintenance requirements, is certainly worth further study.

1.3 "Optimal Control Strategy"

The collector heat removal factor (F_R) relates the actual useful energy gain of a solar collector to the useful gain if the whole collector were at the fluid inlet temperature. It is primarily a function of the mass flow rate of fluid through the collector ($\dot{m}$) [1]:

$$F_R = \frac{\dot{m}C_p(T_o - T_i)}{A_c[S - U_L(T_i - T_a)]} \qquad (1.2)$$

The maximum possible useful energy gain occurs when the entire collector is at the inlet fluid temperature, so that heat losses to the surroundings are minimized.

As the mass flow rate through the collector is increased, the temperature rise across the collector decreases. This causes lower thermal losses since the average collector temperature is reduced, and hence the useful energy gain (Q_u) is increased. Operating an active system pump at a high flow rate does not necessarily mean that the system performance will be improved, however. As the mass flow rate through the collector is increased, the greater amount of recirculation through the storage tank disturbs the stratified temperature profile. The return temperature from the tank bottom to the collector is increased, thus increasing the average collector temperature and the associated thermal losses, which decreases the useful energy gain. These contrary effects of flow rate on Q_u indicate the existence of an optimum flow rate, at which the useful energy gain is maximized.

The solar fraction (F) is used as a measure of thermal performance of a system. In non-dimensional form, it takes into account the useful solar energy gain as well as the load energy requirement, and is defined here as:

$$F = 1 - \frac{Q_{aux}}{Q_{sup}} \tag{1.3}$$

Q_{aux} is the auxiliary energy required, including that needed to

supply tank thermal energy losses, but excluding the parasitic energy needed to operate pumps and automatic valves. Q_{sup} is the energy required to heat the hot water draw from the mains temperature to the supply temperature.

A.B. Copsey [8] investigates the thermal advantage of a storage tank with a stratified temperature profile, over a fully mixed uniform temperature storage tank. Figure 1.8 illustrates the variation of solar fraction with collector flow rate per unit area for two similar active solar DHW systems, one simulated with a stratified storage tank, the other modeled with a fully mixed tank. At very low flow rates, the performance of both systems is similar, due to the marked decrease in F_R. At high flow rates, the performance of the stratified tank system approaches that of the fully mixed tank system, since the large amount of recirculation causes the difference between the tank top and bottom temperatures to be small.

M.D. Wuestling et al. [7] show that the optimum performance of active solar DHW systems occurs when the ratio of monthly average daily collector flow to load flow ($\overline{M_c}/M_L$) is approximately one. Similarly, for thermosyphon solar DHW systems, G.L. Morrison and J.E. Braun [9] show that the optimum performance occurs when the average daily collector volume flow is approximately equal to the daily load volume.

1.3.1 Natural vs. Pumped Circulation

To compare the long term performance of equivalent thermosyphon and active systems, simulations were performed using the TRNSYS

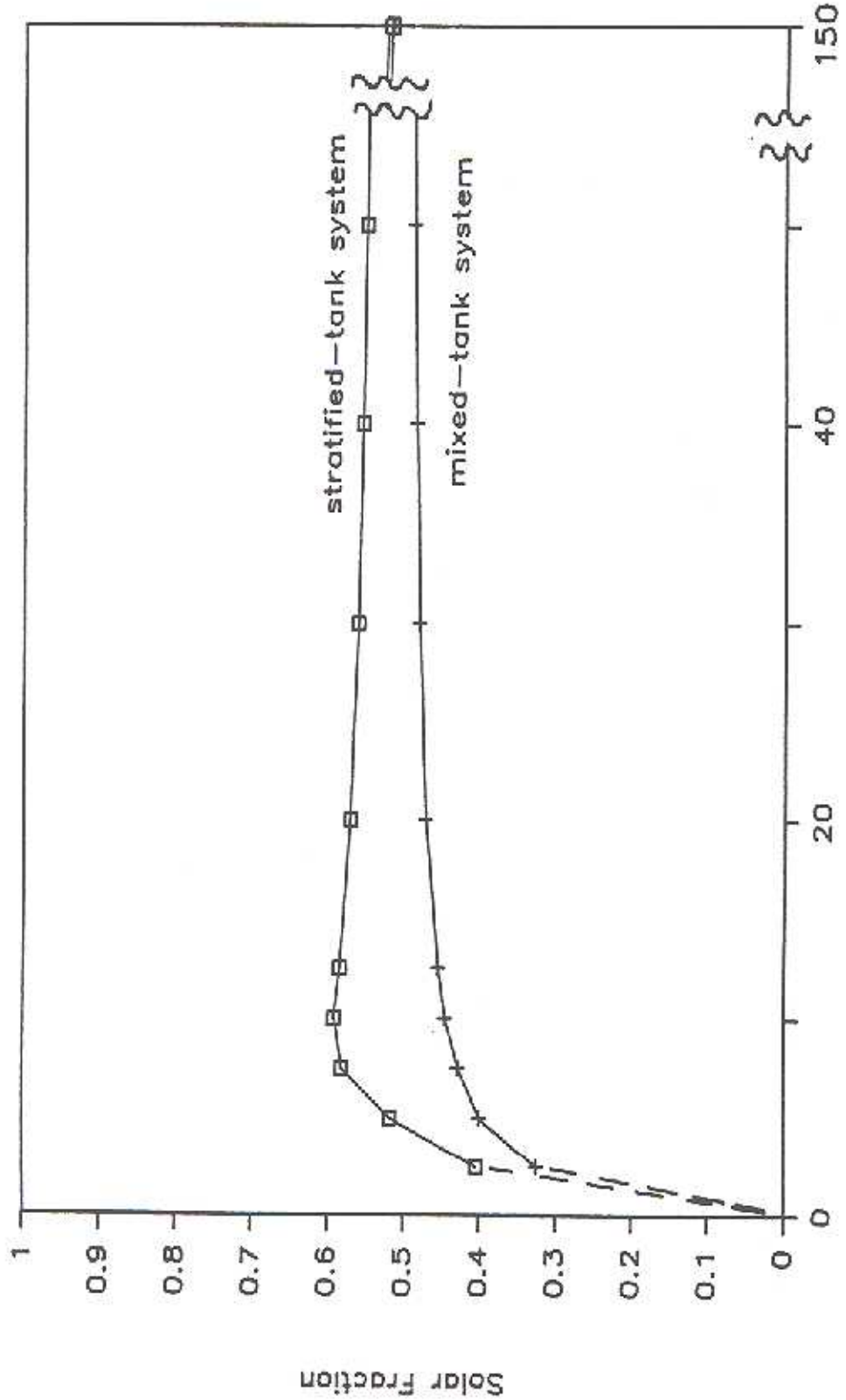

Figure 1.8 Effect of collector flow rate on solar fraction for a stratified tank and a fully mixed tank system.
From A.B. Copsey [8]

Transient System Simulation Program [10] (TRNSYS is discussed in detail in Chapter 2). Weather data for the month of April in Albuquerque, New Mexico, and a daily hot water load draw of 300 liters were chosen to drive the simulations of the 1.4 m^2 collector area systems. The systems were subjected to the RAND load draw profile, which is a "typical" hourly load distribution prepared from data collected in a Rand Corporation survey of residential water heating [11]. A sketch of the RAND load distribution is shown in Figs. 2.6 and 2.7. A range of values for monthly average daily collector flow through the thermosyphon system was obtained by varying the collector riser diameter (frictional resistance) and the height of the storage tank above the collector (thermosyphon head).

Figure 1.9 illustrates the effect of $\overline{M}_C/M_L$ on solar fraction for a thermosyphon system, and two active systems. The two active systems which differ only in the differential controller deadband settings, were operated at a range of fixed low collector flow rates. The differential temperature controller functions to turn the active system pump on whenever the temperature difference between the collector outlet and the bottom of the storage tank is above a certain turn-on deadband, and turn off the pump whenever the difference drops below a certain turn-off level. Two controller deadband settings were chosen for comparison in the simulations. The "perfect" controller, with zero degree turn-on and turn-off levels, allows the collection of all available solar energy, but is not practical due to the excessive cycling of the pump. The controller with an 8.9°C

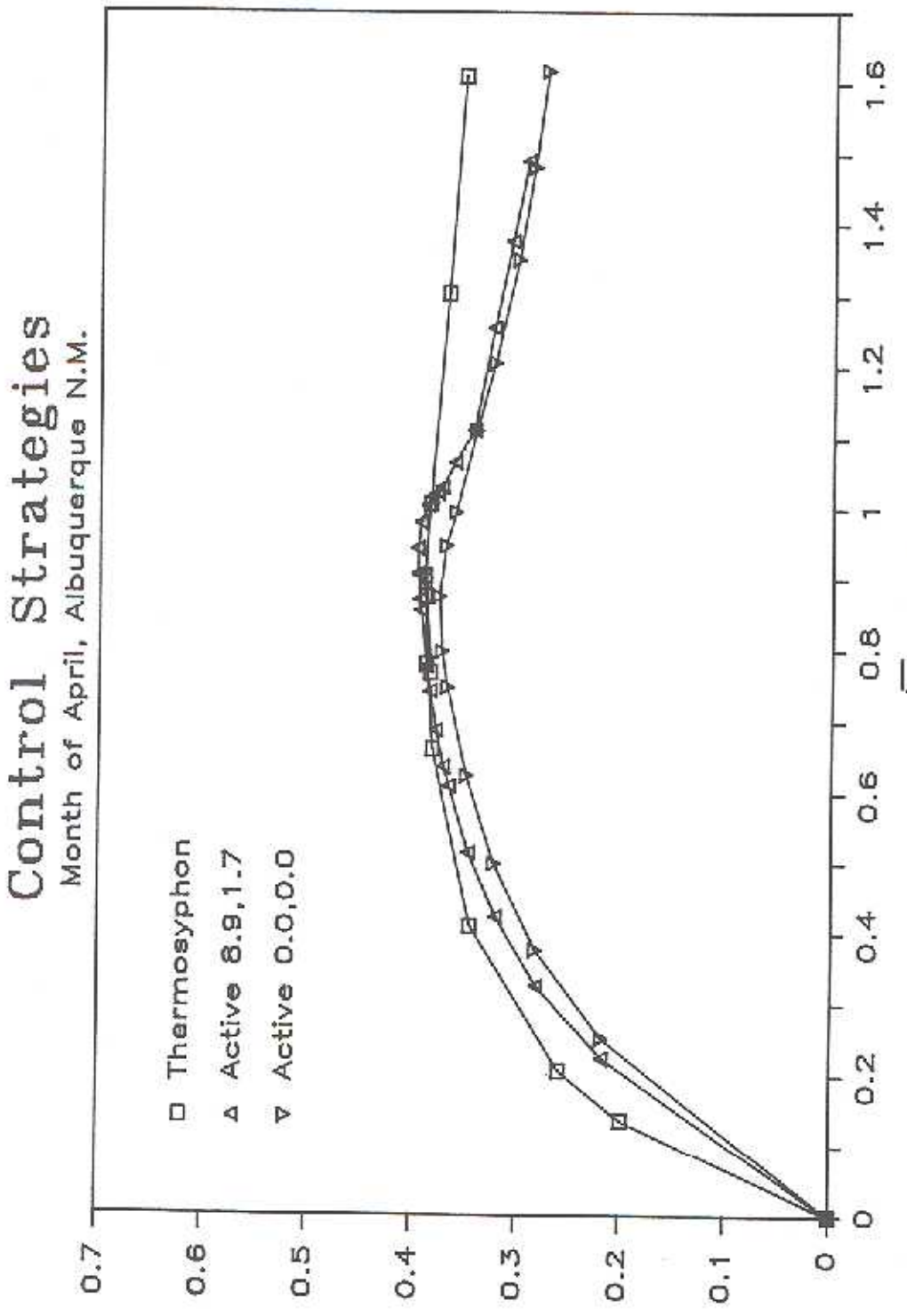

Figure 1.9 Monthly solar fraction as a function of $\bar{M}_c/M_L$ for a thermosyphon and two active system control strategies

turn-on temperature difference and a 1.7°C turn-off level, which employs the same settings as used in the NBS experiment [4], more closely resembles controllers used in practice.

It is interesting to note that the system with an 8.9°C on, 1.7°C off, controller deadband setting performed slightly better than that of the system with the "perfect" 0°C, 0°C differential controller, at the low flow rates under investigation. Although the "perfect" controller permits more energy collection during the sunrise and sunset hours, the negative effect of additional disturbance of the storage tank stratification resulting from the small increase in operation time more than offsets the increased solar gain. Furthermore, since the monthly average ambient temperature for April in Albuquerque is 12°C, and the simulation mains water temperature was set at 12°C, the "perfect" controller allows the pump to circulate fluid through the collector on warm evenings. The small thermal gain during the evenings is not great enough to justify the increased mixing of the storage tank. It may be concluded that a controller setting with finite temperature deadbands (8.9°C, 1.7°C) has an advantage both for practical reasons to reduce pump cycling, and for thermal reasons, over a "perfect" controller. It is possible that for the particular meteorological conditions and system configuration under study, there exists an on/off controller setting which will give slightly better performance than the 8.9°C, 1.7°C deadband.

There is very little difference in the performance between the thermosyphon system and the active system with finite deadband oper-

ated at low collector flow rates. At the optimum $\bar{M}_c/M_L$ ratio, the active system performed slightly better than the thermosyphon system, for the particular size of the systems under the particular conditions of the simulation. At flow rates greater than the optimum, which occur often in practice, the thermosyphon system out performed the active system. It should be noted that the parasitic energy requirement of the pump, which would detract from the active system performance, has not been considered in evaluating the solar fraction.

Thermosyphon systems may be viewed as inherently exhibiting an "optimal control strategy", since the flow rate through the collector varies throughout the day. Around sunrise and sunset, the flow rate is very low, thereby not disturbing the stratified temperature profile in the storage tank. Around noon time, when the solar radiation is high and the advantage of increased energy collection outweighs the disadvantage of recirculating the storage fluid, the flow rate is high. Couple this with the fact that natural circulation thermosyphon systems require no maintenance for a pump and controller, and they begin to look even more attractive.

1.4 Review of Thermosyphon Modeling Literature

Numerous studies have been conducted to investigate the transient temperatures and flow rates throughout the day in thermosyphon systems. The following is a brief summary of some of the prior literature on thermosyphon system modeling.

D.J. Close [12] develops a simple analytical model for predicting the daily performance of a thermosyphon system under the conditions of clear sunshine and no load draw. Using an energy balance on the entire system, Close develops a differential equation describing the time variation of the average storage tank temperature. The solution to the differential equation under the simplifying conditions of sinusoidal time variations of solar radiation and ambient temperature yields an analytical model.

C.L. Gupta and H.P. Garg [13] modify the model of Close to take into account the heat exchange efficiency of the collector absorber plate, and thermal capacitance. The solar radiation and ambient temperature are represented by using Fourier series expansions. These modifications make the Close model valid for cloudy weather also. However, the simplifying condition of no load draw during the period of analysis is still retained.

K.S. Ong [14,15] extends the work of Close and Gupta and Garg by using a finite difference solution procedure, and a different formulation of the absorber plate efficiency factor. The model considers the system to be broken up into a finite number of sections, with each section having a uniform temperature. Ong simulates and measures the mass flow rate, mean tank temperature, and collector efficiency using actual solar radiation and ambient temperature data.

J.W. Baughn and D.A. Dougherty [16] modify the model of Ong by including a more detailed model of the collector, and the transition of flow from laminar to turbulent. A "thermal analyzer program", de-

signed for solving complex transient conduction, convection, and radiation problems using the resistance-capacitance analogy, is used to speed up the computation in Ong's model.

M.S. Sodha and G.N. Tiwari [17] analyze the transient performance of thermosyphon systems based on the formulation of Ong, except that provision is made in the storage tank energy balance equation for a hot water load draw.

Y. Zvirin et al. [18] outline a method of solving the differential energy equation and coupled momentum equation to obtain a steady state temperature distribution and flow rate. The model can serve only as an approximation for the behavior of a system around noon time.

G.L. Morrison and D.B.J. Ranatunga [19,20] investigate the response of thermosyphon systems to step changes in solar radiation. Measurement of the transient flow rate is obtained using a laser doppler anemometer, and a mathematical model is developed to simulate the transient performance.

B.J. Huang [21] solves a dimensionless form of the energy and momentum equations using a finite difference technique. Ten dimensionless groups which characterize the system are derived and the effects of tank height, tank volume, solar radiation, and flow resistance, on flow rate are studied. Huang assumes no load draw, constant ambient temperature, no thermal losses from the connecting pipes, and only laminar flow in the system.

A. Mertol et al. [22] develop an analytical model to analyze the performance of a thermosyphon water heater with a heat exchanger in the storage tank. Mertol et al. use a similar technique as Huang, except they consider load draw, transient heat transfer in the connecting pipes, and both laminar and turbulent flow in the system.

G.L. Morrison and J.E. Braun [9] develop an efficient numerical simulation model for thermosyphon solar water heaters. The model is compatible with the widely used TRNSYS simulation program [10] and is discussed in detail in Chapter 2.

1.4.1 Long Term Performance

Although the literature contains many studies of transient effects in thermosyphon systems, very little work has been published concerning the long term system performance. G.L. Morrison and C.M. Sapsford [23] experimentally measure the fractional energy savings provided by six different thermosyphon system setups in Sydney, Australia from December 1980 - November 1981. The aim of the experiments is to be able to predict the average performance of a particular system over its expected life in Sydney. Since the solar radiation and environmental conditions during a particular test are unlikely to match the long term average conditions, Morrison and Sapsford develop a model that describes the system performance and calibrate the model using the particular data obtained during the tests. The correlation has limited application, however, since it is developed for a specific location and system configuration.

In Chapter 3 a general design method, developed over a broad range of systems in a variety of locations, is discussed. The design method allows the prediction of the annual performance of a wide array of thermosyphon solar DHW systems.

CHAPTER 2: DETAILED MODEL USING TRNSYS

TRNSYS is a transient system simulation program which is used for thermal analysis of a variety of time dependent systems. The modular nature of TRNSYS permits the simulation of a great variety of thermal systems. The modular components are mathematical models of the particular components of a physical system. Typical components of an active solar heating system are solar collectors, pipes, pump, controller, heat exchanger, valves, storage tank, auxiliary energy heater, loads, etc. A typical thermosyphon solar DHW system as used in practice may be modeled by connecting the thermosyphon collector storage subsystem (TRNSYS Type 45) with a mixing valve (Type 11), optional in-line auxiliary energy heater (Type 6), weather data (Types 9, 16), and heating load components (Types 14 and 15). A schematic representation of the flow of information into and out of each of the components of the thermosyphon system under investigation is shown in Fig. 2.1. Each component is represented as a box which requires a number of constant parameters, and time dependent inputs. Outputs from the box are calculated by the equations describing the component. The particular system configuration being studied may be altered by changing the interconnections between the various components. A complete TRNSYS deck for modeling a thermosyphon water heating system with an in-line auxiliary heater appears in Appendix A.

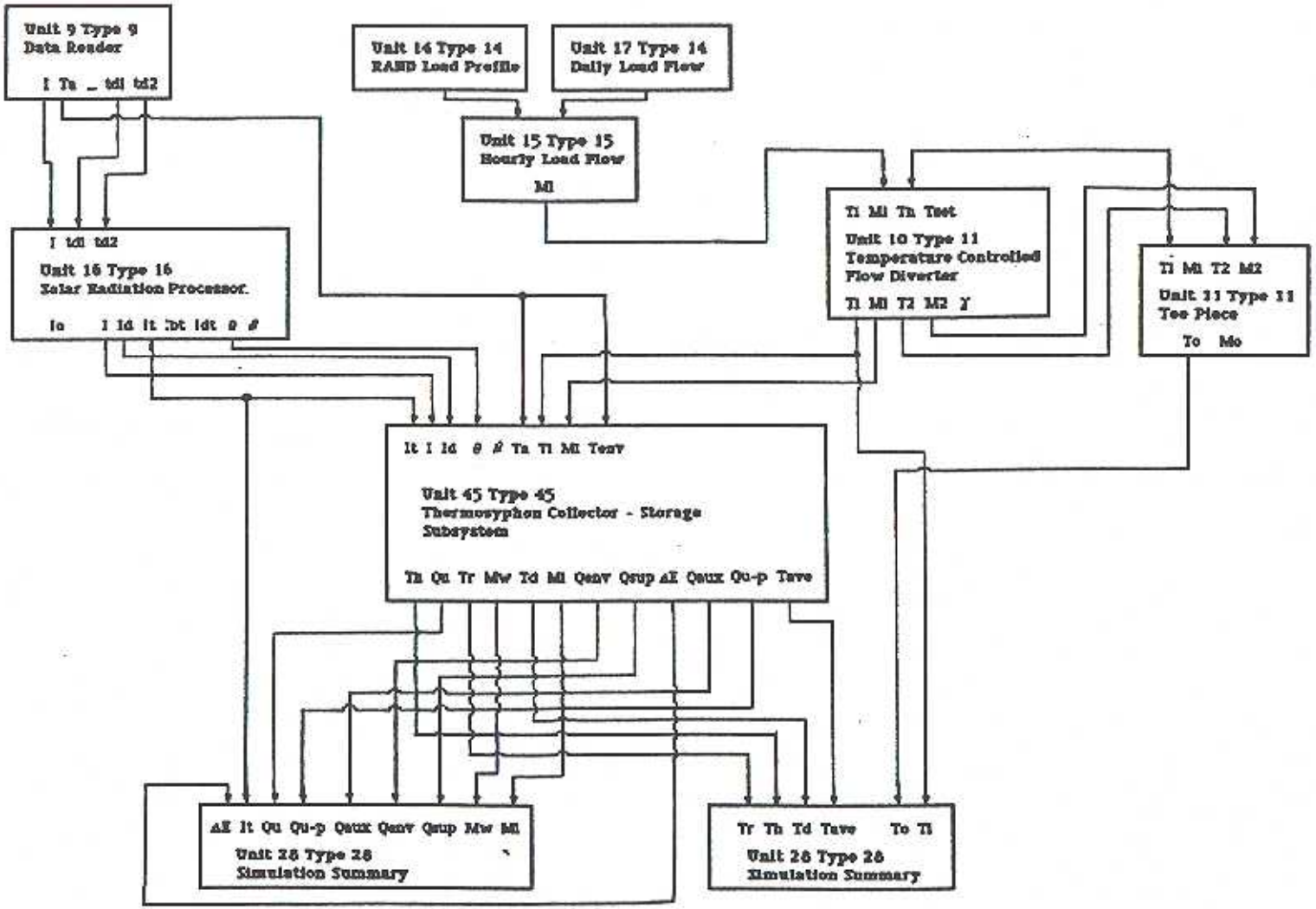

Figure 2.1 TRNSYS information flow diagram for a thermosyphon system

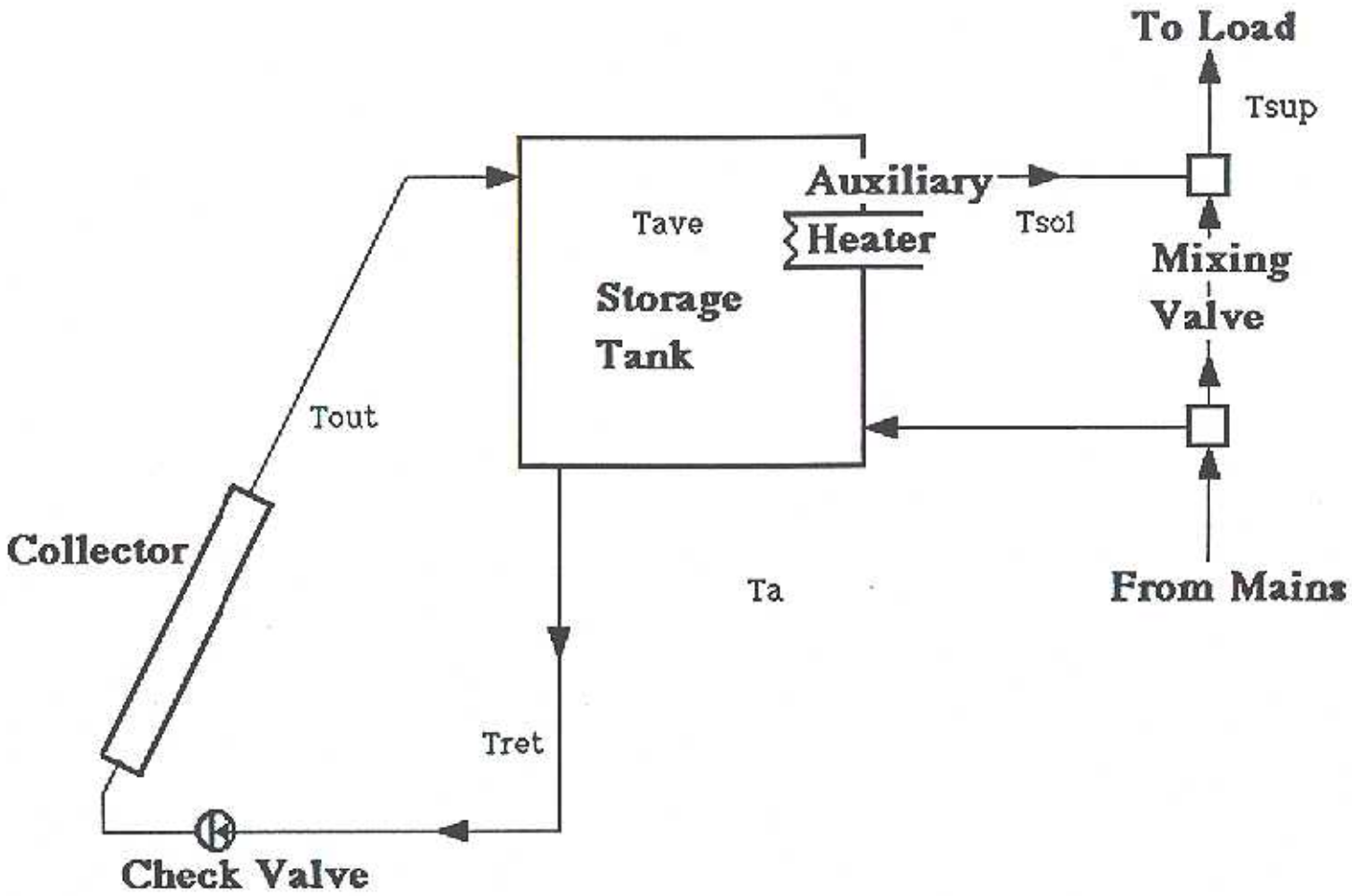

Figure 2.2 Schematic diagram of a thermosyphon system

2.1 TRNSYS Utility Components

Several component models termed utility components, have been previously formulated for inputting data and performing mathematical manipulations for simulation of most any transient system. In general, these components do not have physical counterparts in actual hardware.

2.1.1 TMY Data Reader

TRNSYS component Type 9 is used to read hourly values of solar radiation incident on a horizontal surface (I) and ambient temperature (T_a) for the Typical Meteorological Year (TMY) at a particular location. The TMY data base was created by Hall et al. [24] through a study of 23 years of data for each of 26 stations in the United States solar radiation network.

2.1.2 Solar Radiation Processor

TRNSYS component Type 16 transforms the TMY hourly radiation incident on a horizontal surface into radiation incident upon a flat plate collector at a fixed slope with respect to the horizontal. The total horizontal radiation is broken down into its beam and diffuse parts, and then transformed to beam and diffuse fractions on the specified tilted surface. A correlation developed by D.G. Erbs [25] is used to estimate the diffuse fraction of total horizontal radiation (I_d/I) as a function of the clearness index ($k_T = I/I_0$). Beam radiation on the horizontal surface is the difference between the total radiation and the diffuse part ($I_b = I - I_d$). The beam radiation on the horizontal is transformed to beam radiation on the

tilted surface through a series of geometric relationships involving latitude (ϕ), collector tilt angle (β), collector azimuth angle (γ), declination angle (δ), and hour angle (ω) [1]. The diffuse radiation on the tilted surface, as well as the ground reflected radiation, is a function of collector tilt, and is assumed to be isotropic.

2.1.3 RAND Load Draw

Two units of TRNSYS Type 14 (Time Dependent Forcing Function) and one Type 15 (Algebraic Operations) are combined to simulate the RAND hourly hot water load draw for a specified total daily load flow.

2.2 Mixing Valve

A mixing valve is included in the system to mix solar heated water with colder mains water if the solar heated water temperature is above the set temperature. This prevents overheating and unnecessary use of the energy in the storage tank. For simulation purposes, the mixing valve comprises two parts, a tee piece and a temperature controlled flow diverter (TRNSYS Types 11, Modes 1 and 4 respectively).

2.3 Thermosyphon Collector Storage Subsystem

The thermosyphon collector storage combined subsystem (TRNSYS Type 45) comprises a flat plate solar collector, connecting piping, check valve to prevent reverse flow, and a stratified storage tank, in a single mathematical model. Since the system models direct

circulation, water is specified as the working fluid. The system is analyzed by dividing the thermosyphon loop into a number of segments normal to the flow direction and applying Bernoulli's equation for incompressible flow to each segment. For steady state conditions, the pressure drop in any segment is:

$$\Delta P = \rho_i g h_{Fi} + \rho_i g H_i \qquad (2.1)$$

where h_{Fi} is the friction head loss through an element and H_i is the height of the element. For each time interval, the model numerically solves for the collector flow rate that balances the frictional head loss with the head due to density differences, so that $\Delta P = 0$. The fluid density is evaluated at the local temperature using a correlation for water.

2.3.1 Collector

The collector thermal performance is modeled on the basis of the Hottel-Whillier equation, by dividing it into N_k equally spaced nodes. The temperature at the midpoint of any collector node k is:

$$T_k = T_a + \frac{I_T F_R U_L}{F_R(\tau\alpha)} + \left(T_i - T_a - \frac{I_T F_R U_L}{F_R(\tau\alpha)}\right) e^{-(F'U_L A_c (K-1/2))/(\dot{m} C_p N_k)} \qquad (2.2)$$

The collector parameter $F'U_L$ is calculated from the ASHRAE 93-77 test value of $F_R U_L$ at the collector test flow rate ($\dot{m}_{test}$):

$$F'U_L = -\frac{\dot{m}_{test}}{A_c} C_p \ln\left(1 - \frac{F_R U_L A_c}{\dot{m}_{test} C_p}\right) \quad (2.3)$$

This procedure neglects changes in F' and U_L with flow rate and temperature. The parameter $F_R(\tau\alpha)$ is determined from the ASHRAE 93-77 intercept efficiency at normal incidence and separate incidence angle modifiers for beam, diffuse, and ground reflected radiation [26]. The overall useful energy gain from the collector is:

$$Q_u = rA_c[F_R(\tau\alpha)I_T - F_R U_L(T_i - T_a)] \quad (2.4)$$

where

$$r = \frac{F_R U_L}{F_R U_L}\bigg|_{use}^{test} = \frac{F_R(\tau\alpha)}{F_R(\tau\alpha)}\bigg|_{use}^{test} = \frac{\dot{m}\left(1 - e^{-F'U_L A_c/\dot{m}C_p}\right)}{\dot{m}_{test}\left(1 - e^{-F'U_L A_c/\dot{m}_{test}C_p}\right)} \quad (2.5)$$

2.3.2 Connecting Pipe

The connecting pipes between the collector and tank are modeled as single nodes with negligible thermal capacitance. The pipe outlet fluid temperature is given by:

$$T_{po} = T_a + (T_{pi} - T_a)\, e^{-(UA)_p/\dot{m}C_p} \quad (2.6)$$

2.3.3 Stratified Storage Tank

Thermal stratification in the storage tank is modeled with a "plug flow" tank model (TRNSYS Type 38). The "plug flow" model uses

a number of variable sized constant temperature segments of fluid to simulate thermal stratification. A description of its operation is illustrated in Fig. 2,3, in which a series of temperature profiles are plotted vs. the vertical position in the tank. The top profile represents an initial temperature distribution at time T_1. If a collector flow occurs during the timestep, a uniform temperature segment of fluid, whose size depends on the collector flow rate, is inserted into the tank profile at the tank inlet. With the fixed inlet mode, any temperature inversions resulting from the fluid inlet are removed by mixing the newly inserted segment with adjacent segments. The position of the segments below the inlet are shifted downwards. If a load flow occurs during the timestep, a "plug" of fluid at the mains temperature and equal in volume to the load flow is inserted at the bottom of the tank, shifting the temperature profile upwards. The segments outside the bounds of the tank are returned to the collector and/or load, and the process is repeated for the following timestep. The return temperatures are calculated as volume weighted averages. Storage tank thermal losses are then calculated individually for each segment of fluid in the temperature profile.

The advantage of this tank model is that small fluid segments are introduced when stratification is developing, while zones of uniform temperature, such as above an in-tank auxiliary heater, are represented by large fluid segments. The size of the fluid segments used to represent the tank thermal stratification varies with the collector flow rate [9]. The "plug flow" tank model does not solve a

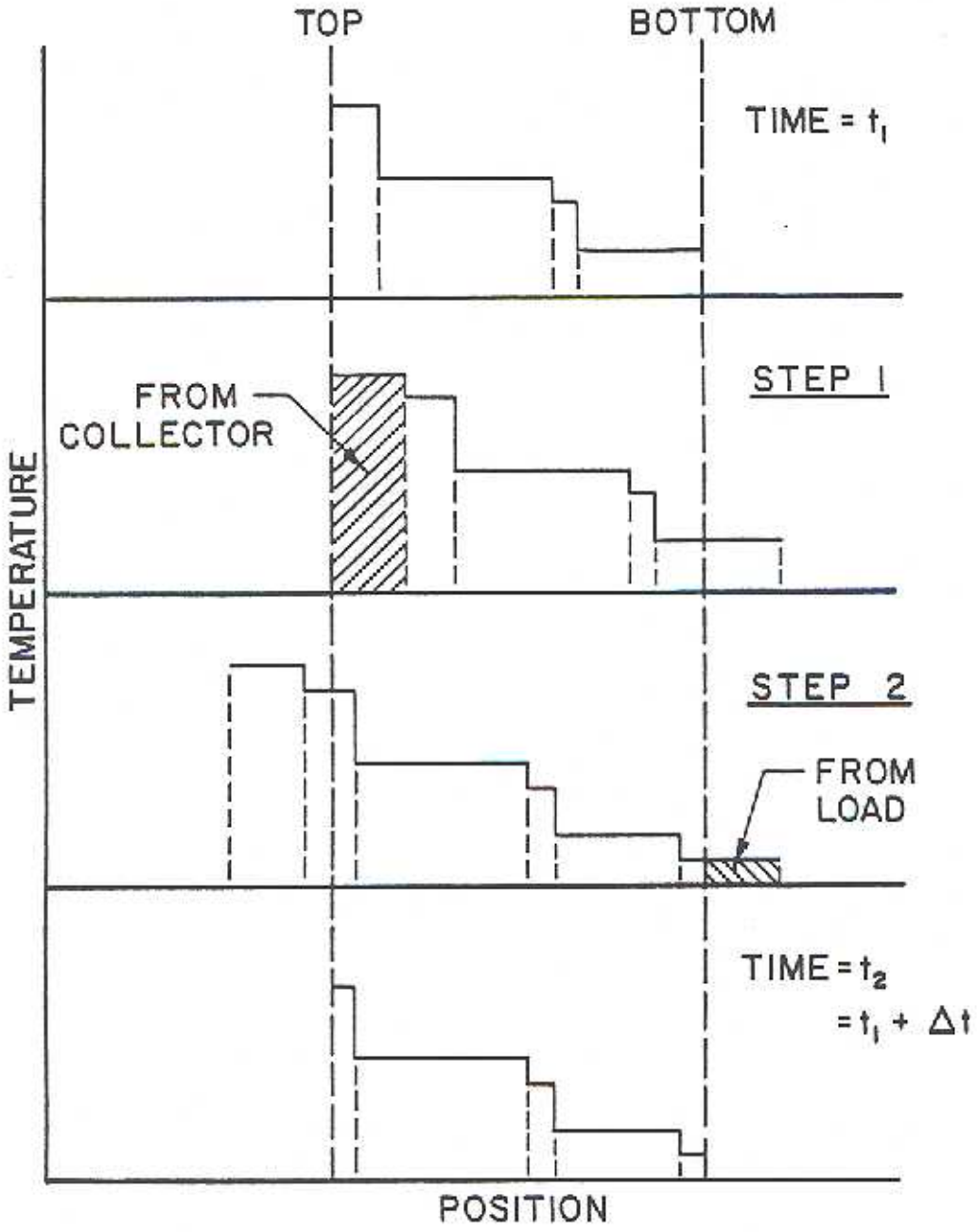

Figure 2.3 Operation of "plug flow" storage tank model. From M.D. Wuestling [27]

set of simultaneous equations and is therefore computationally more efficient than a finite difference multi-node stratified tank model (TRNSYS Type 4).

Conduction between the fluid segments may be optionally considered. Morrison and Braun [9] suggest that conduction be included in horizontal tank systems with an in-tank auxiliary heater. The loss of performance due to conduction is primarily caused by conduction from the top auxiliary zone into the lower tank segments. The short conduction path in horizontal tanks results in significant heating of the lower segments, reducing the degree of thermal stratification. Table 2.1 shows the effect of conduction in various tank geometries without an in-tank auxiliary heater. For annual solar fractions around 70%, in a vertical tank with height/diameter of 2.7, conduction affects less than a 1% reduction in solar fraction, while in a long horizontal tank (length/diameter = 5.4) conduction causes a 3% reduction. Although the effect of conduction is more prominent in horizontal than vertical tanks, on the basis of Table 2.1 conduction may be neglected for all reasonable tank geometries without an in-tank auxiliary heater in systems with annual solar fractions less than 70%.

2.4 Comparison with NBS Experiment

Comparison between TRNSYS simulation results and measurements taken at the National Bureau of Standards in Gaithersburg, Maryland on one particular thermosyphon system is shown in Table 2.2. Excel-

TABLE 2.1: Effect of Conduction on System Performance in Storage Tanks of Various Geometries

Tank Type	H/D or L/D	Solar Fraction	
		No Conduction	With Conduction
Vertical	2.7	0.404 0.718	0.402 0.713
Squat	1.0	0.407 0.721	0.404 0.710
Horizontal	2.7	0.408 0.722	0.404 0.703
Horizontal	5.4	0.409 0.722	0.403 0.698

TABLE 2.2: Comparison of Experimental Results at the National Bureau of Standards and TRNSYS Simulation of a Thermosyphon System

Date 1980	Measured Load MJ/day	Measured Auxiliary MJ/day	Measured f_r^*	Simulation Load MJ/day	Simulation Auxiliary MJ/day	Simulation f_r^*
Jan	907	630	0.43	929	655	0.42
Feb	1095	446	0.65	1096	510	0.63
Mar	1530	796	0.55	1514	883	0.52
Apr	990	284	0.75	946	278	0.76
May	1164	403	0.71	1195	423	0.71
June	1099	299	0.77	1165	312	0.79
July	913	198	0.82	896	164	0.85
Aug	604	216	0.72	617	226	0.71
Sep	950	270	0.78	978	218	0.83
Oct	781	382	0.61	792	314	0.68
Nov	1670	1033	0.46	1590	969	0.5
Dec	483	265	0.54	471	264	0.53
Annual	12187	5222	0.65	12188	5219	0.65

f_r^* = fractional energy savings relative to conventional system with tank loss of 11.6 MJ/day

From G.L Morrison and J.E Braun [9]

lent agreement between the simulation and measurements was found for both annual delivered load and annual auxiliary energy consumption.

The system consisted of three collector panels mounted in parallel, with each panel of 1.4 m^2 aperture area, 10 parallel risers of 4.93 mm diameter, $F_R(\tau\alpha) = 0.805$, $F_R U_L = 4.73$ W/m^2-°C, $K\tau\alpha = 1 - 0.1(1/\cos\theta - 1)$. The ASHRAE 93-77 collector parameters were obtained at a test flow rate of 0.02 $kg/m\text{-}sec^2$. The collectors were connected by 25 mm ID pipes to a 242 liter storage tank with an overall energy loss coefficient (UA) of 1.47 W/°C. A check valve was included to prevent reverse thermosyphon flow. The system performance was measured from January-December 1980, while a daily load of 250 liters was withdrawn according to the RAND distribution. An in-tank auxiliary electrical heater was controlled by a thermostat with a set temperature of 63°C and a 14°C deadband.

2.5 Process Dynamics

Figures 2.4-2.9 illustrate the process dynamics from TRNSYS simulations of two systems similar in configuration to the NBS system described earlier. Figures 2.4 and 2.5 show energy quantities, Figs. 2.6 and 2.7 flow rates, and Figs. 2.8 and 2.9 temperatures, characteristic of the systems. The only difference between the pair of systems is the number of collector panels. Figures 2.4, 2.6, and 2.8 are for a one panel system (1.4 m^2), while Figs. 2.5, 2.7 and 2.9 are for a system with two 1.4 m^2 panels connected in parallel (2.8 m^2 total aperture area). The TMY data for April 16 in Albuquerque, New

Mexico was chosen to drive the system, for no reason other than to coincide with the date of the author's first seminar presentation at the U.W. Solar Energy Lab. The one panel system gives a solar fraction of 45% for the day and 38% for the month of April in Albuquerque, while the two panel system gives a daily solar fraction of 80% and a monthly value of 72%.

Insight into the operation of thermosyphon systems may be gained by not only analyzing the energy, flow rate, and temperature process dynamics of one system, but also comparing the corresponding plots of the pair of systems.

2.5.1 Energy

Figures 2.4 and 2.5 illustrate the energy quantities representative of the one panel and two panel systems respectively. The curve labeled "A" is the solar radiation incident on the collector surface (I_T). The solar radiation is seen to vary throughout the day, approximately symmetric about solar noon. Curve "B" represents the useful solar energy gain from the collector, neglecting thermal losses from the collector - tank connecting pipe (Q_u). The variation of the useful energy gain throughout the day follows the same form as the varying insolation incident on the collector. A measure of the efficiency of solar energy collection may be obtained by dividing Q_u by I_T. Curve "C" represents the useful energy gain when connecting pipe thermal losses of 4.6 W/m^2-°C are included (Q_u-P). Curve "C" is barely discernible from curve "B", indicating that the thermal losses from the connecting piping are small. The jagged shape of curve "D"

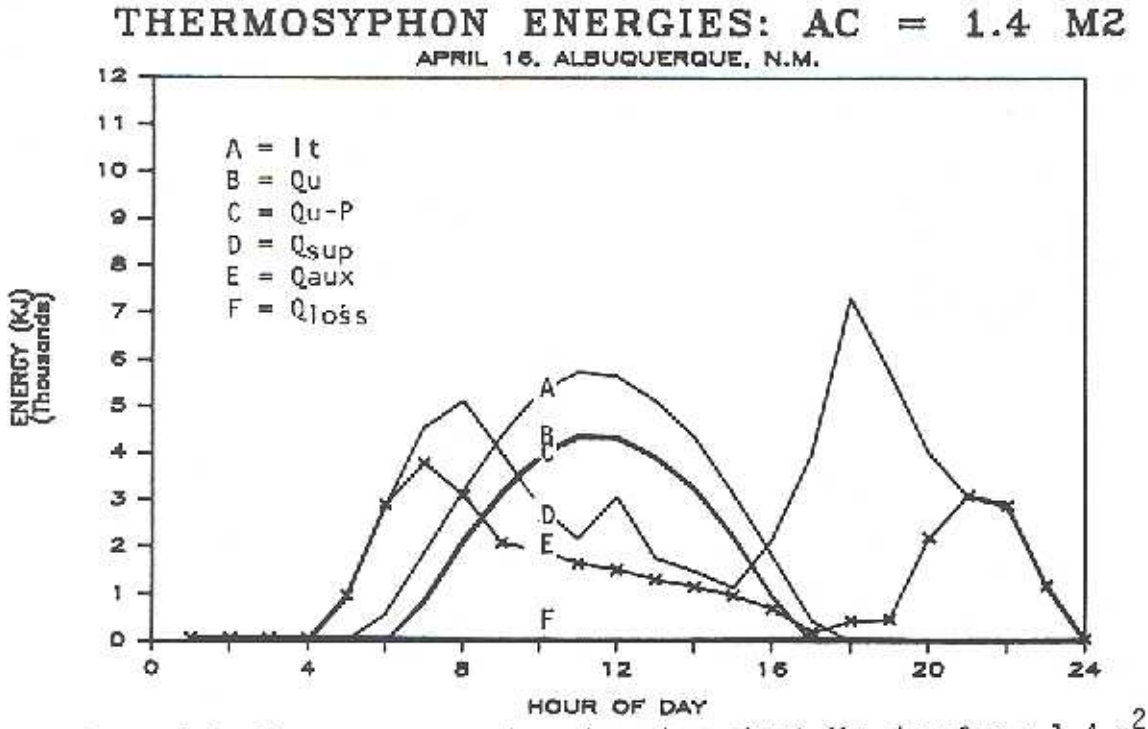

Figure 2.4 Energy process dynamics throughout the day for a 1.4 m^2 collector area thermosyphon system

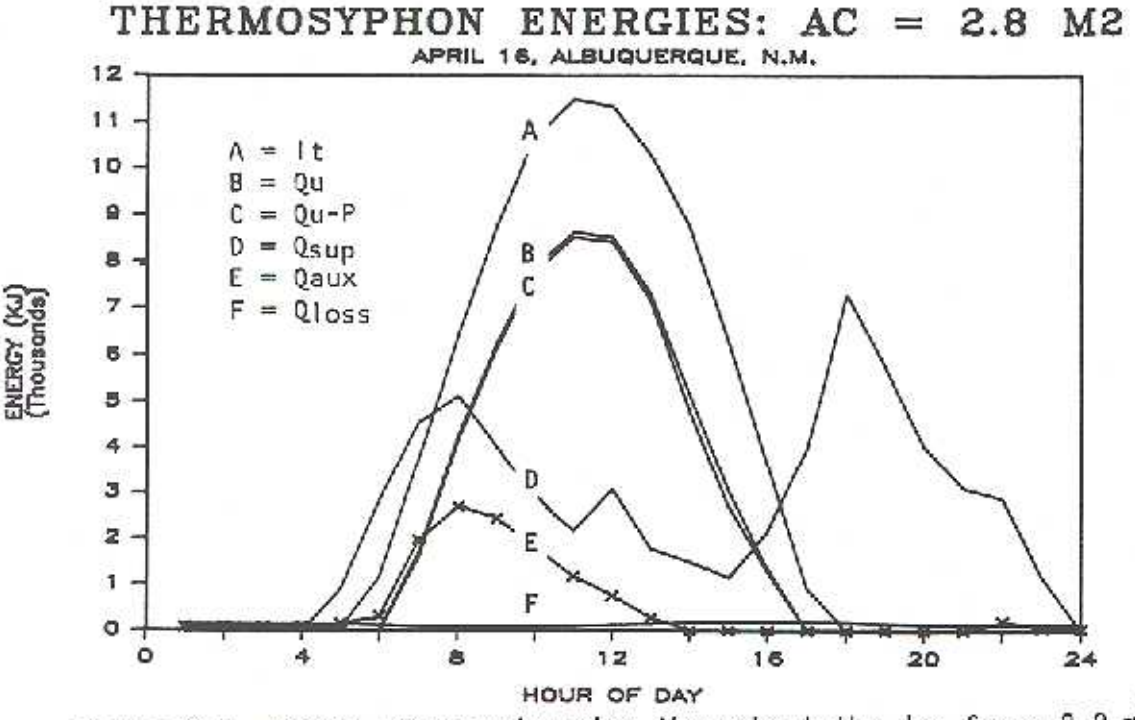

Figure 2.5 Energy process dynamics throughout the day for a 2.8 m^2 collector area thermosyphon system

represents the energy content of the 60°C water supplied to load (Q_{sup}) according to the RAND distribution. Curve "E" represents the auxiliary energy required by the electrical in-tank heater to meet the desired load of 60°C water (Q_{aux}). The auxiliary heater is required in both systems to meet the morning peak load, although to a lesser extent in the two panel system. A substantial amount of auxiliary energy is also needed to meet the evening load in the one panel system, while the two panel system meets the evening peak almost wholly by solar energy. This is due to the greater amount of solar energy collection throughout the day, and greater amount of energy stored in the storage tank, of the two panel system. Curve "F" represents the thermal losses from the storage tank to the ambient air with UA value of 1.46 W/°C (Q_{loss}). The greater tank loss in the two panel system is due to the higher average temperature of the water in the storage tank.

2.5.2 Flow Rate

Figure 2.6 illustrates how the flow rate through the collector in the one panel system follows the form of the solar radiation incident on the collector. As the radiation increases from 6 A.M. to noon, the water in the collector loop heats up. As the collector fluid becomes warmer and hence less dense than the fluid in the storage tank, the buoyancy driving force is increased. As the radiation decreases in the afternoon, the collector fluid temperature decreases, which decreases the buoyancy force, and hence the flow rate

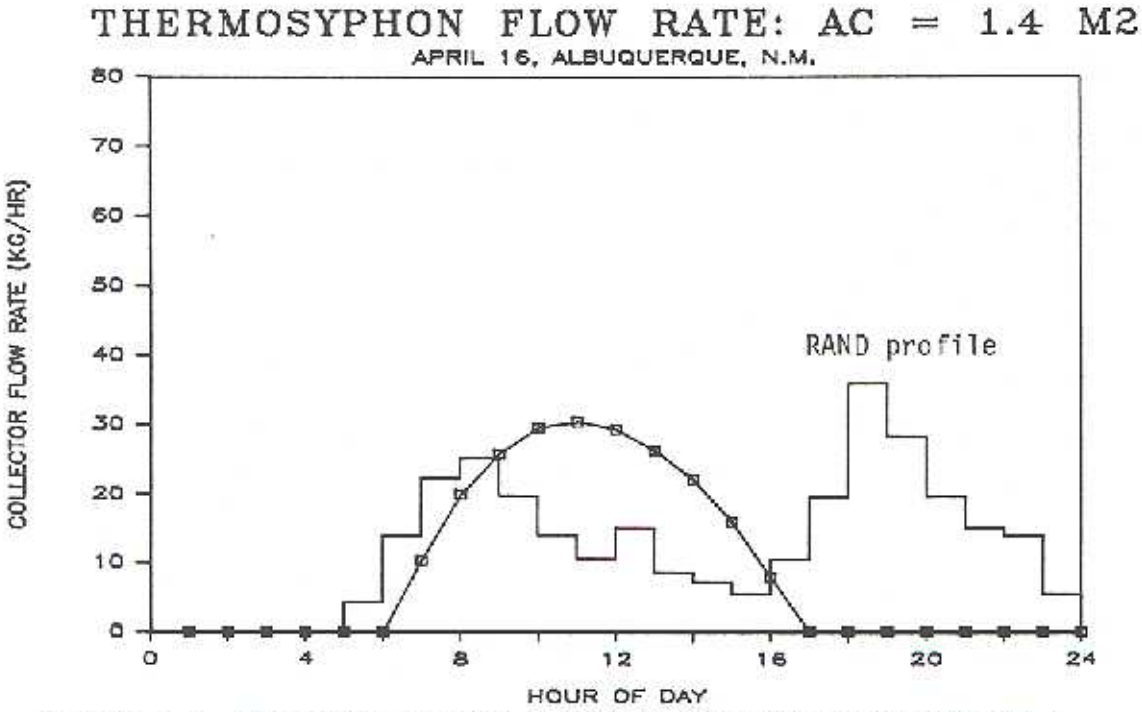

Figure 2.6 Flow rate process dynamics throughout the day for a 1.4 m^2 collector area thermosyphon system

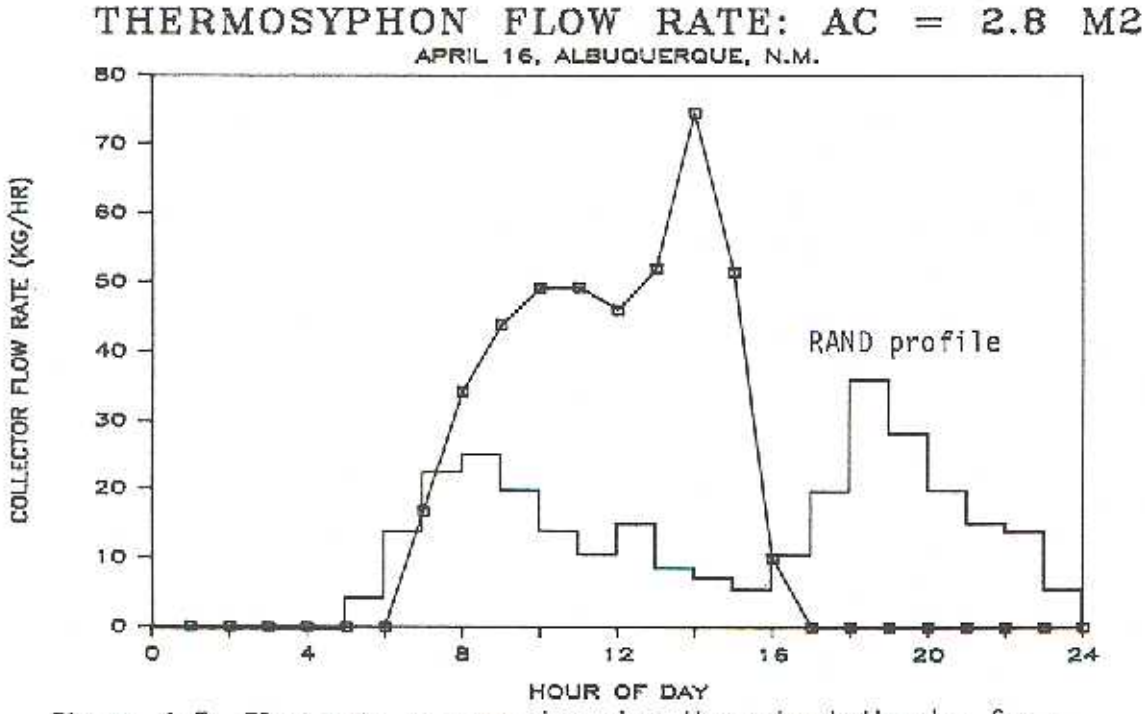

Figure 2.7 Flow rate process dynamics throughout the day for a 2.8 m^2 collector area thermosyphon system

is reduced. A discretized form of the RAND hourly load flow distribution is also shown on both Figs. 2.6 and 2.7.

The collector flow rate profile for the two panel system shown in Fig. 2.7 is not as intuitive as for the one panel system. As might be expected, the flow rate between the hours of 6 A.M. to noon is greater in the two panel system than in the one panel system, due to the larger collector area receiving greater incident radiation. However, the flow rate profile does not follow the radiation profile in the afternoon hours in the two panel system. A dramatic increase in flow through the collector occurs between 1 and 2 P.M., creating a "blip" in the profile in Fig. 2.7. This "blip" results from the storage tank losing its stratified temperature profile at that hour. Cold water at mains temperature is no longer available at the bottom of the storage tank for return to the collector. The warmer, less dense collector inlet water flows at a higher rate even with the lower incident radiation during the hour, than does colder water with the previous hour's higher radiation. The explanation of this non-intuitive flow profile points out the need for looking at the collector and tank system as a whole, since the temperatures in the storage tank will affect the temperature and flow rate of water through the collector. The beneficial effect of increased flow rate on collection efficiency, and detrimental effect of increased collector thermal losses due to the higher collector inlet temperature, offset to result in a slight decrease in collection efficiency around 1 P.M.

This decreased efficiency is very slight however, and is not detectable from the curves of I_T and Q_u in Fig. 2.5.

2.5.3 Temperature

The temperature variation throughout the day at six points in the one and two panel systems is shown in Figs. 2.8 and 2.9 respectively. The temperatures correspond to the locations of the abbreviations (T_{ret}, T_{out}, ...) in the schematic drawing, Fig. 2.2. Curve "A" represents the temperature of the water supplied from the top of the storage tank to the mixing valve (T_{sol}). In the one panel system, T_{sol} remains constant at the auxiliary heater set temperature of 60°C. In the two panel system, T_{sol} surpasses the set temperature at 1 P.M., due to the large amount of solar input and small load draw between the noon and 4 P.M. hours. The overheating of the water demonstrates the need for including a mixing valve in the system, to limit the temperature of the hot water delivered to load, and to save the excess energy in the tank for later use. Curve "B" represents the temperature of the water at the outlet of the mixing valve supplied to the load (T_{sup}). The presence of the auxiliary heater and mixing valve keeps the supply temperature constant at the set temperature of 60°C throughout the day. Curve "C" represents the temperature of fluid at the collector outlet (T_{out}). As might be expected, in the one panel system the collector outlet temperature varies throughout the day in the same fashion as the incident radiation. The two panel system shows the expected increase in collector outlet temperature before noon, and the unexpected increase from 1-2 P.M.

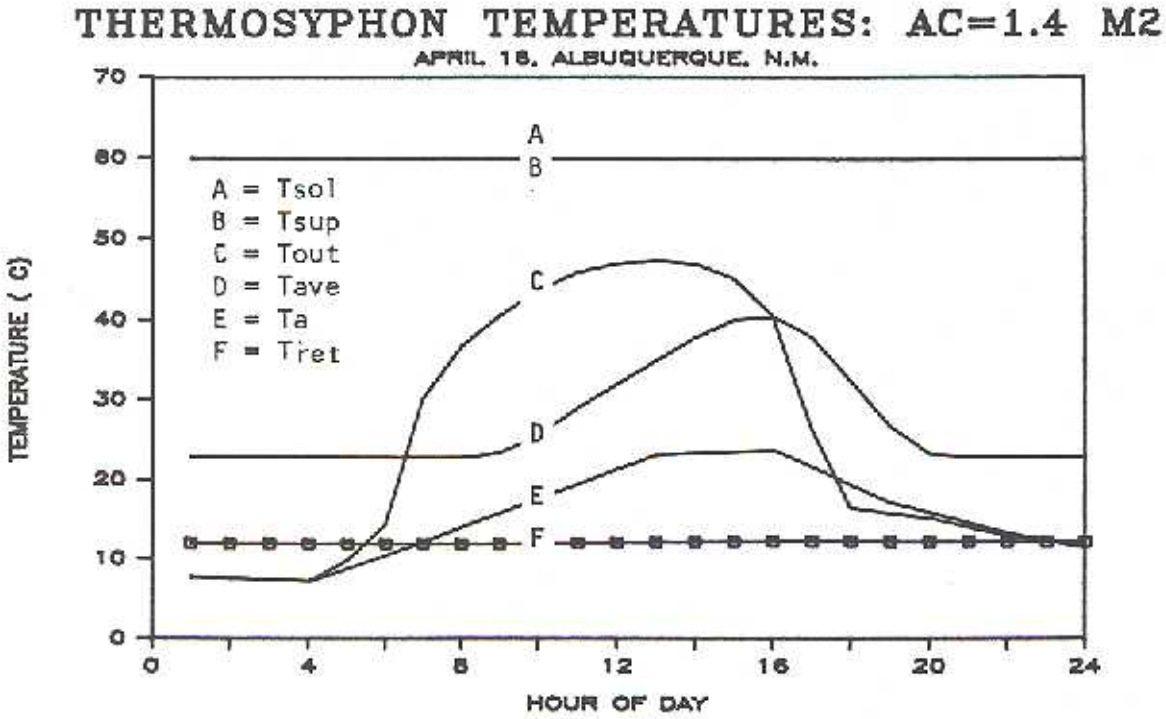

Figure 2.8 Temperature process dynamics throughout the day for a 1.4 m^2 collector area thermosyphon system

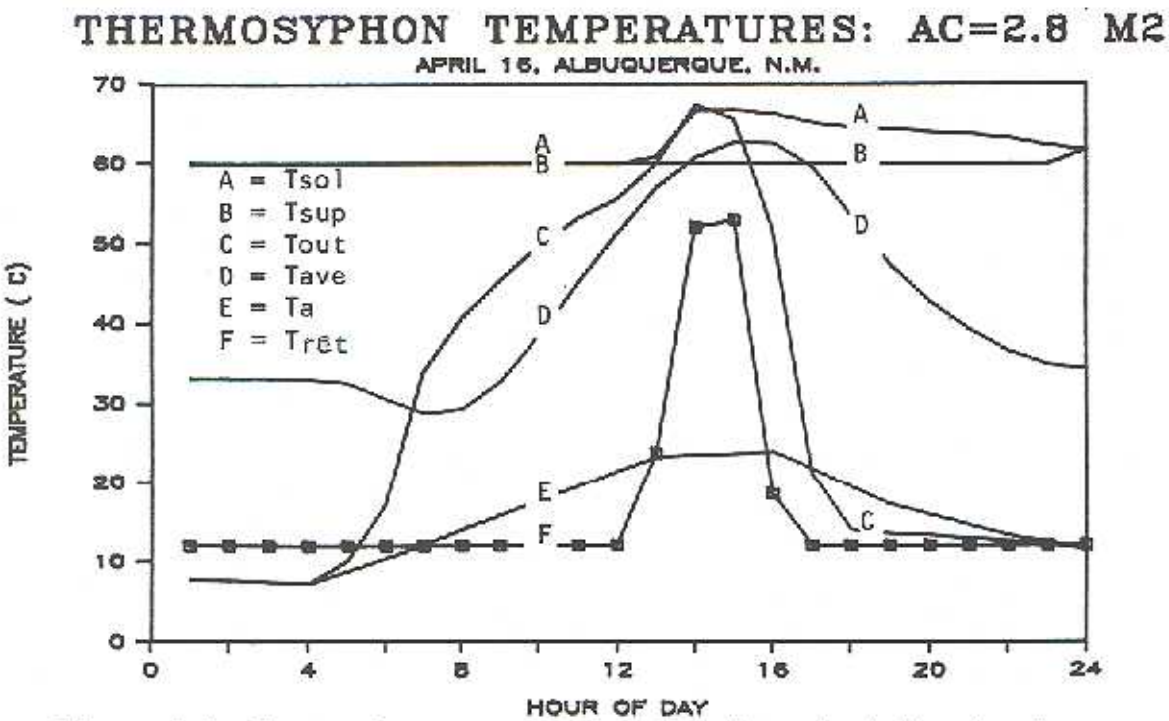

Figure 2.9 Temperature process dynamics throughout the day for a 2.8 m^2 collector area thermosyphon system

due to the abrupt increase in the collector inlet temperature. Curve "D" illustrates the average temperature in the storage tank (T_{ave}). The average storage tank temperature follows a form similar to the ambient temperature (T_a) shown in curve "E". The average storage temperature of the two panel system is greater than that of the one panel system due to the increased amount of useful solar energy gain from the collector (Q_u-P). Curve "F" represents the return temperature of water from the tank to the collector (T_{ret}). By neglecting the connecting pipe thermal losses, this is also the temperature at the collector inlet. In the one panel system, the storage tank remains stratified throughout the day and T_{ret} remains constant at the mains water temperature of 12°C. In the two panel system, the tank stratification is disturbed and the return temperature is increased above the mains water temperature, as previously explained.

The detailed TRNSYS simulations, which require hourly meteorological data, are useful for understanding the process dynamics of a system. However, even with the computational efficiency of the "plug flow" tank model, an annual simulation of a thermosyphon solar DHW system requires a substantial amount of computing time. As a result, detailed simulations are not practical as a design tool for estimating the monthly and annual performance of a variety of thermosyphon solar DHW system configurations. In Chapter 3, a design procedure based on the f-Chart method [28] for estimating the long term performance of thermosyphon systems is discussed in detail.

CHAPTER 3: DESIGN METHOD FOR THERMOSYPHON SYSTEMS

The f-Chart method is a widely used design tool for estimating long term performance of forced circulation solar heating systems. It requires only monthly average meteorological data and system parameters as inputs. In its present form, the f-Chart method is not appropriate for estimating the performance of thermosyphon systems for two reasons. First, the f-Chart method was developed for active systems with a fixed known flow rate of fluid through the collector. Second, the f-Chart method assumes that the storage tank is in a fully mixed state (uniform temperature at any time), which is a reasonable assumption for systems operating at normal high collector flow rates. As mentioned earlier, recent experiments and simulations have shown that optimum performance for active systems may be achieved with a flow rate on the order of 1/5 of the normal rates. Thermosyphon systems usually operate in the low flow range, and hence exhibit thermally stratified tanks.

The f-Chart method may be modified to enable prediction of the improved performance of systems exhibiting stratified storage tanks. Furthermore, the varying flow through the thermosyphon system may be approximated by an "equivalent average" fixed flow rate for each month in an active system. The active system operating at this fixed flow rate will yield similar results for monthly fractional energy savings by solar as the thermosyphon system. Thus, the long term

performance of a thermosyphon system may be predicted using a modified form of the f-Chart method, as described below.

3.1 Stratified Tank Modification

Thermally stratified storage tanks return fluid to the collector at a temperature below that of the average temperature in the storage tank. As mentioned earlier, this results in increased collection efficiency by reducing thermal losses from the collector. A.B. Copsey [8] develops a modification to the f-Chart method to account for a stratified storage tank. Copsey shows that the solar fraction for a stratified tank system can be obtained by analysis of an otherwise identical fully mixed tank system with a reduced collector loss coefficient, (U_L). The collector heat removal factor (F_R) is a function of the collector loss coefficient and the collector flowrate, hence a modification to the f-Chart method that is based on the collector loss coefficient will also require modification of F_R. The f-Chart method for DHW systems includes the collector losses in the X parameter, and the heat removal factor in both the X and Y parameters:

$$X = \frac{A_c F_R U_L (11.6 + 1.18\ T_{set} + 3.86\ T_{mains} - 2.32\ \bar{T}_a)\ \Delta t}{L} \qquad (3.1)$$

$$Y = \frac{A_c F_R (\overline{\tau\alpha})\ \bar{H}_T N}{L} \qquad (3.2)$$

The line AB on the liquid system f-Chart in Fig. 3.1 illustrates the

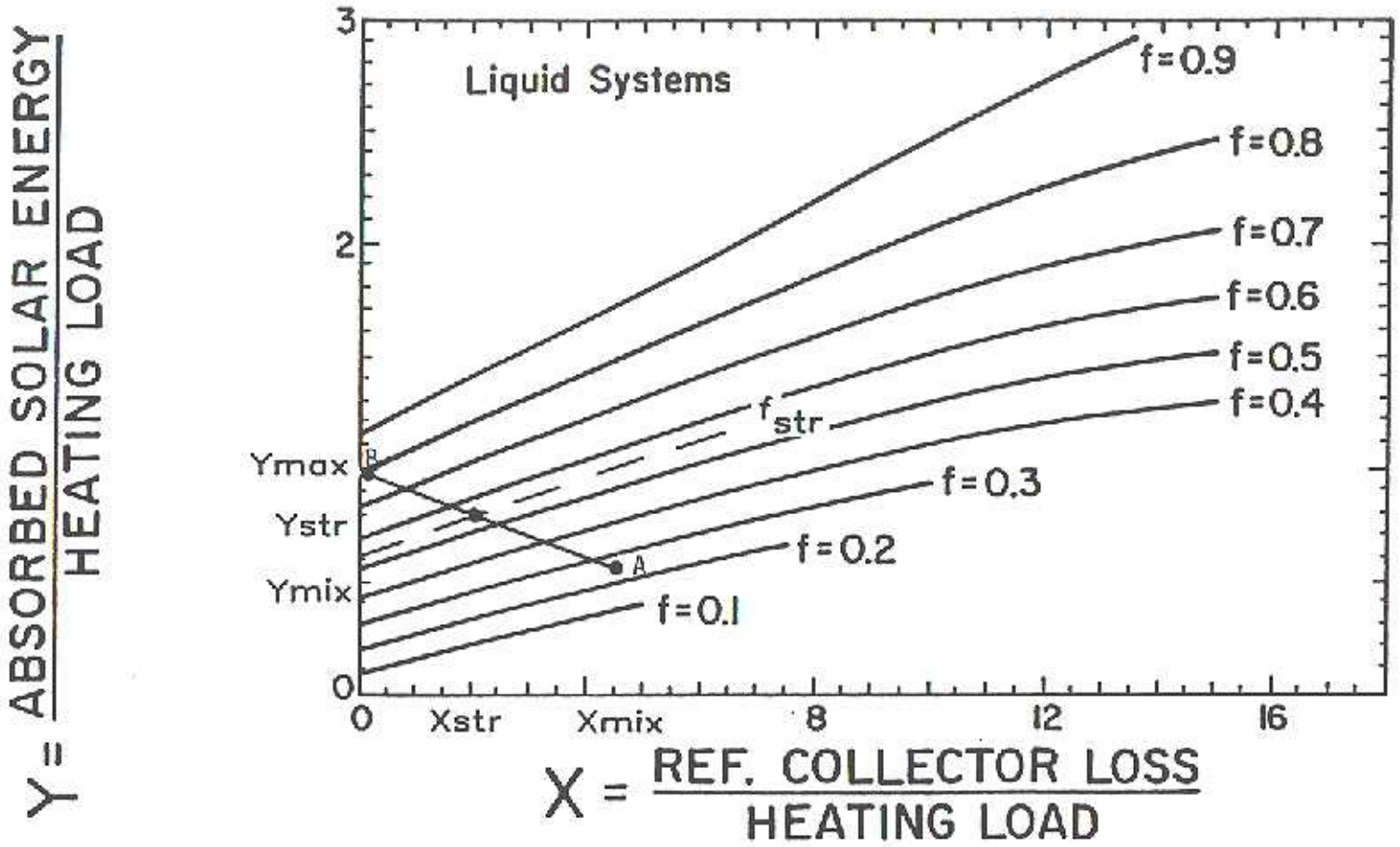

Figure 3.1 Liquid system f-Chart showing the relationship between the f-Chart parameters for a collector with no thermal losses, a system with a stratified storage tank, and a system with a fully mixed storage tank.
From A.B. Copsey [8]

path taken by decreasing the collector losses, while simultaneously modifying F_R (slightly exaggerated for emphasis). The point to the lower right is the location on the liquid system f-Chart of a fully mixed tank system. The mixed tank solar fraction can be obtained from the f-Chart with coordinates X_{mix} and Y_{mix}. If the collector had no thermal losses, then the X parameter would be zero, and the Y parameter would be:

$$Y_{max} = \frac{A_c(\overline{\tau\alpha})\ \overline{H}_T N}{L} \tag{3.3}$$

where $F_R = 1$. The solar fraction for a stratified tank system will always be between the limits of the solar fraction for a fully mixed tank system with the actual collector loss coefficient, and a fully mixed tank system with $U_L = 0$.

If the path shown in Fig. 3.1 is approximated by a straight line, a relationship between the f-Chart parameters can be expressed as:

$$\frac{\Delta X}{\Delta X_{max}} = \frac{X_{mix} - X_{str}}{X_{mix}} = \frac{Y_{str} - Y_{mix}}{Y_{max} - Y_{mix}} \tag{3.4}$$

The relationship $\Delta X/\Delta X_{max}$ is shown by Copsey to be a function of the monthly average collector to load flow ratio ($\overline{M}_c/M_L$) and mixed tank solar fraction (F):

$$\frac{\Delta X}{\Delta X_{max}} = \frac{C_1 (\bar{M}_c/M_L)}{[C_2 (\bar{M}_c/M_L) + C_3 F + C_4 F^2]^2 + 1} \qquad (3.5)$$

The coefficients C_1-C_4 that minimize the RMS error between TRNSYS simulations of a stratified tank active system and the f-Chart method modified for stratified storage are C_1 = 1.040, C_2 = 0.726, C_3 = 1.564, and C_4 = -2.760. Due to the nature of Eq. (3.5), a high solar fraction combined with $\bar{M}_c/M_L$ near one, can give $\Delta X/\Delta X_{max} > 1$. For these cases $\Delta X/\Delta X_{max}$ should be set equal to one.

3.1.1 Pump Operating Time

The number of hours that the active system collector pump operates is needed to calculate the daily mass of fluid that is pumped through the collector (M_c). J.C. Mitchell et al. [29] show that the pump operating time (N_p) with a zero degree differential temperature controller may be expressed as:

$$N_p = -\bar{H}_T \frac{d\bar{\Phi}}{dI_c} \qquad (3.6)$$

where $\bar{\Phi}$ is the monthly average daily utilizability, I_c is the critical radiation level, and $\bar{H}_T$ is the solar radiation incident on the collector. Utilizability is defined as the fraction of the incident solar radiation that can be converted to useful heat (i.e., utilized) by a collector having $F_R(\tau\alpha) = 1$, and operating at a fixed collector inlet temperature to ambient temperature difference [1]. Although the collector has no optical losses and has a heat removal factor of

one, the utilizability is always less than one since the collector has thermal losses from the top, sides, and back of the collector panel. D.L. Evans et al. [30] develop an empirical relationship for the monthly average daily utilizability as a function of the critical radiation level, the monthly average clearness index ($\bar{K}_T$), the collector tilt (β), and the latitude (ϕ):

$$\bar{\Phi} = 0.97 + A\bar{I}_c + B\bar{I}_c^2 \tag{3.7}$$

where:

$$A = -4.86 \times 10^{-3} + 7.56 \times 10^{-3}\, \bar{k}_T' - 3.81 \times 10^{-3}\, (\bar{k}_T')^2 \tag{3.8}$$

$$B = 5.43 \times 10^{-6} - 1.23 \times 10^{-5}\, \bar{k}_T' + 7.62 \times 10^{-6}\, (\bar{k}_T')^2 \tag{3.9}$$

for:

$$\bar{k}_T' = \bar{k}_T \cos\left[0.8\,(\beta_m - \beta)\right] \tag{3.10}$$

where β_m is the monthly optimal collector tilt, shown in Table 3.1. Differentiating Eq. (3.7) and substituting into Eq. (3.6) yields an expression for the monthly average daily collector pump operating time:

$$\bar{N}_p = -\bar{H}_T\,(A + 2B\bar{I}_c) \tag{3.11}$$

TABLE 3.1: Collector Tilt Angle for Optimum Monthly Incident Energy

Month	β_m (degrees)
January	ϕ + 29
February	ϕ + 18
March	ϕ + 3
April	ϕ - 10
May	ϕ - 22
June	ϕ - 25
July	ϕ - 24
August	ϕ - 10
September	ϕ - 2
October	ϕ + 10
November	ϕ + 23
December	ϕ + 30

*Collector is assumed to be facing south (γ = 0) in the Northern Hemisphere.

From D.L. Evans et al. [30]

The monthly average critical radiation level is defined as the level above which useful energy may be collected:

$$\bar{I}_c = \frac{F_R U_L (\bar{T}_i - \bar{T}_a)}{F_R(\overline{\tau\alpha})} \qquad (3.12)$$

In order to find the monthly average critical radiation level, a value for the monthly average collector inlet temperature ($\bar{T}_i$) must be known. $\bar{T}_i$ cannot be determined analytically, and as illustrated in Fig. 2.9 it may vary in an unpredictable manner. The collector inlet temperature is a function of the thermal stratification in the storage tank and, as discussed later, may be approximated using Phillips' stratification coefficient. Under the assumption that the storage tank remains stratified, the monthly average collector inlet temperature may initially be estimated to be the mains water temperature.

Once Copsey's modification has accounted for the stratified tank, the problem of varying flow rate in a thermosyphon system may be addressed.

3.2 "Equivalent Average" Flow Rate

The varying flow rate in a thermosyphon system may be approximated by an "equivalent average" fixed flow rate in an active system. An iterative scheme has been developed for estimating this flow rate for use with the f-Chart method modified for stratified storage, to

allow prediction of the long term performance of thermosyphon systems.

Using an initial estimated value for flow rate, the solar fraction of a stratified tank active system is evaluated using the f-Chart method with Copsey's modification for stratified storage. The collector parameters $F_R U_L$ and $F_R(\tau\alpha)$ are corrected for the estimated flow at other than test conditions as outlined in Section 2.3.1, by the coefficient (r). Thermal losses from the connecting pipes, however slight, may be accounted for as outlined in Duffie and Beckman [1]. The combination of pipes plus solar collector is equivalent in thermal performance to a solar collector with parameters $F_R(\tau\alpha)'$ and $F_R U_L'$:

$$\frac{(\tau\alpha)'}{(\tau\alpha)} = \frac{1}{\left(1 + \frac{U_p A_o}{\dot{m} C_p}\right)} \tag{3.13}$$

$$\frac{U_L'}{U_L} = \frac{1 - \frac{U_p A_i}{\dot{m} C_p} + \frac{U_p (A_i + A_o)}{A_c F_R U_L}}{1 + \frac{U_p A_o}{\dot{m} C_p}} \tag{3.14}$$

where U_p is the thermal loss coefficient of the pipe, and A_i and A_o are the surface areas of the collector inlet and outlet connecting pipes respectively.

3.2.1 Storage Tank Average Temperature

The average temperature in the storage tank is calculated using a correlation developed between solar fraction of a thermosyphon

system and a non-dimensional form of the monthly average tank temperature, deduced from numerous TRNSYS simulations, shown in Fig. 3.2. A variety of locations (Albuquerque, NM; Madison, WI; Seattle, WA), collector areas (1.4-4.2 m^2), load draws (300-600 liters/day), tank sizes (125-500 liters), and collector parameters ($F_R(\tau\alpha)$ 0.7-0.8, $F_R U_L$ 3.6-8.6 W/m^2-°C) were included in the correlation. The correlation was developed under the assumption of a constant overall loss coefficient (UA) for the storage tank of 1.46 W/°C. A cubic equation for the data from a least squares regression routine is:

$$\frac{\bar{T}_{tank} - T_{mains}}{T_{set} - T_{mains}} = 0.117\ F + 0.356\ F^2 + 0.424\ F^3 \qquad (3.15)$$

3.2.2 Stratification Coefficient

The temperature at the bottom of the storage tank will be between the mains temperature (T_{mains}) and the average tank temperature ($\bar{T}_{tank}$), depending on the degree of thermal stratification present. An approximate measure of the stratification may be obtained using the stratification coefficient (K_s) defined W.F. Phillips and R.N. Dave [31]:

$$K_s = \frac{A_c[F_R(\tau\alpha)I_T - F_R U_L(T_i - T_a)]}{A_c[F_R(\tau\alpha)I_T - F_R U_L(T_{tank} - T_a)]} \qquad (3.16)$$

Although Phillips and Dave's study assumes zero load draw on the system and more than one tank turnover per day, it will provide a rough estimate of the temperature profile in the tank, and hence of

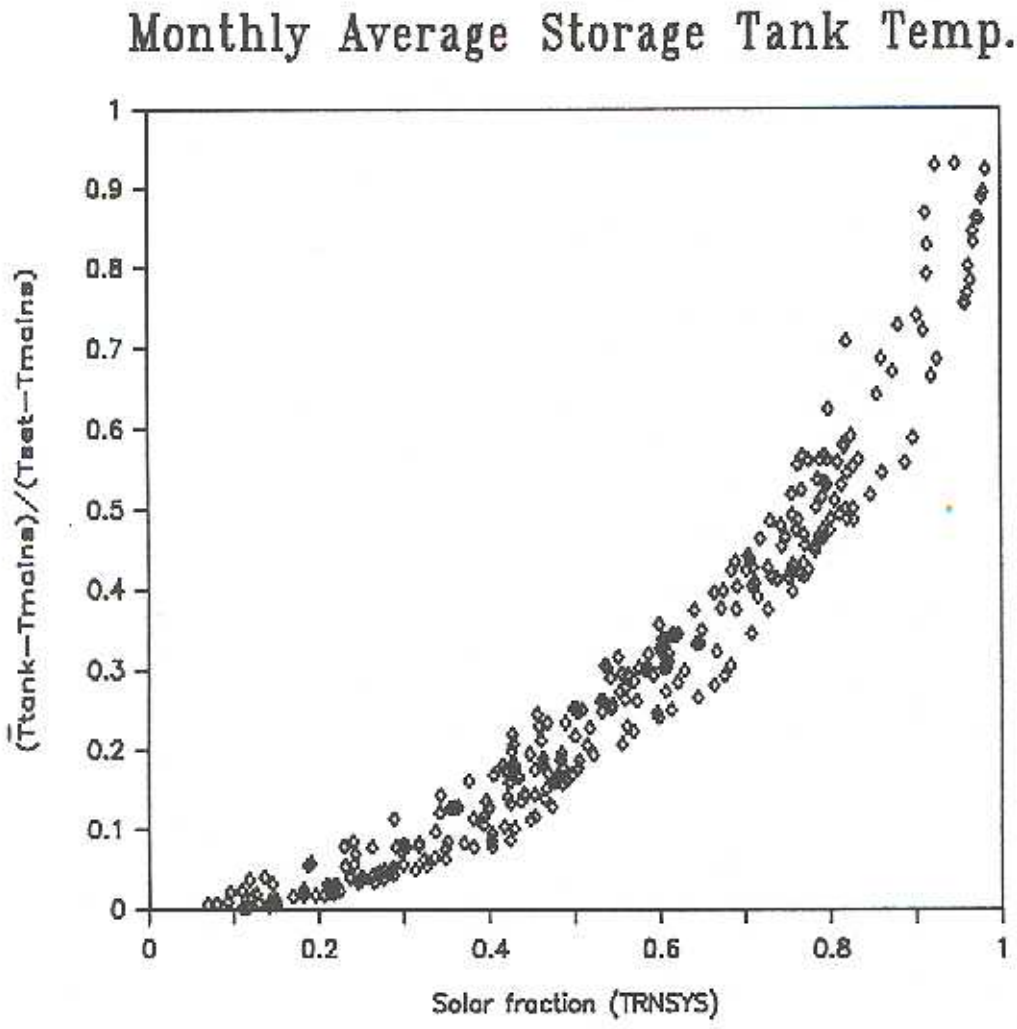

Figure 3.2 Monthly average storage tank temperature (non-dimensionalized) as a function of monthly solar fraction for a thermosyphon system

the temperature of fluid returned to the collector. The stratification coefficient is a function of two dimensionless variables, the mixing number (M) and the collector effectiveness (E):

$$M = \frac{A_s K}{\dot{m} C_{ps} H} \tag{3.17}$$

$$E = \frac{F_R U_L}{\dot{m} C_p} \tag{3.18}$$

Physically, the mixing number is the ratio of conduction to convection in the storage tank. In the limit as conduction in the tank becomes negligible, and (M) approaches zero, Phillips and Dave show that:

$$K_s = \frac{\ln\left(\frac{1}{1 - E}\right)}{E\left(1 + M \ln\left(\frac{1}{1 - E}\right)\right)} \tag{3.19}$$

The temperature of the return fluid from tank to collector may be found from Eq. (3.16):

$$T_i = K_s T_{tank} + (1 - K_s)\left(\frac{F_R(\tau\alpha)}{F_R U_L} I_T + T_a\right) \tag{3.20}$$

Using the estimate of pump operating time from Eq. (3.11), the monthly average temperature of return fluid is approximated as:

$$\overline{T}_i = K_s \overline{T}_{tank} + (1 - K_s)\left(\frac{F_R(\overline{\tau\alpha})}{F_R U_L (N_p)} \overline{H}_T + \overline{T}_a\right) \tag{3.21}$$

Since the thermal loss from the tank-collector connecting pipe has already been accounted for by the modified collector parameters in Eqs. (3.13) and (3.14), $\bar{T}_i$ is also the monthly average collector inlet temperature. For values of $\bar{T}_i$ calculated by Eq. (3.21) less than T_{mains}, $\bar{T}_i$ is set equal to T_{mains}. The collector outlet temperature at the estimated flow rate is found from the definition of the heat removal factor shown in Eq. (1.2). By rearranging and integrating Eq. (1.2) for a monthly period, and letting $S = \bar{H}_T(\overline{\tau\alpha})$, the monthly average collector fluid outlet temperature ($\bar{T}_o$) may be expressed as:

$$\begin{aligned} \bar{T}_o &= \bar{T}_i + \frac{A_c}{\dot{m}C_p\bar{N}_p}\left[\bar{H}_T F_R(\overline{\tau\alpha}) - F_R U_L(\bar{N}_p)(\bar{T}_i - \bar{T}_a)\right] \\ &= \bar{T}_i + \frac{A_c}{\dot{m}C_p\bar{N}_p}\left[\bar{\Phi}\,\bar{H}_T\,F_R(\overline{\tau\alpha})\right] \end{aligned} \tag{3.22}$$

3.2.3 Thermosyphon Head

Once the monthly average collector fluid inlet and outlet temperatures are known, an estimate of the thermosyphon head may be found based on the relative positions of the tank and collector. Close [12] has shown that the thermosyphon head generated by the differences in density of fluid in the system may be approximated by making the following assumptions:

1 - There are no thermal losses in the connecting pipes.

2 - Water from the collector rises to the top of the tank.

3 - The temperature distribution in the tank is linear.

$$h_T = \frac{1}{2}(S_i - S_o)\left[2(H_3 - H_1) - (H_2 - H_1) - \frac{(H_3 - H_5)^2}{(H_6 - H_5)}\right] \quad (3.23)$$

where S_i is the specific gravity of the fluid at the collector inlet, S_o the specific gravity at the collector outlet, and the positions H_1-H_6 as shown in Fig. 3.3. The design method described in this paper considers only direct circulation thermosyphon systems where water is the collection fluid. A parabolic relationship between specific gravity of water and temperature in degrees Celsius is used to calculate S_i and S_o [10],

$$S = 1.0026 - 3.906 \times 10^{-5}\, T - 4.05 \times 10^{-6}\, T^2 \quad (3.24)$$

3.2.4 Frictional Resistance

The "equivalent average" flow rate is that which balances the thermosyphon buoyancy force with the frictional resistances in the flow circuit on a monthly average basis. The flow circuit comprises the collector headers and risers, connecting pipes, and storage tank. For each component of the flow circuit, the Darcy-Weisbach equation for friction head loss is employed [12]:

$$h_F = \frac{f l\, u^2}{2gd} + \sum \frac{k u^2}{2g} \quad (3.25)$$

where f is the friction factor = 64/Re for laminar flow in pipes where Re < 2000, and f = 0.032 for turbulent flow where Re > 2000.

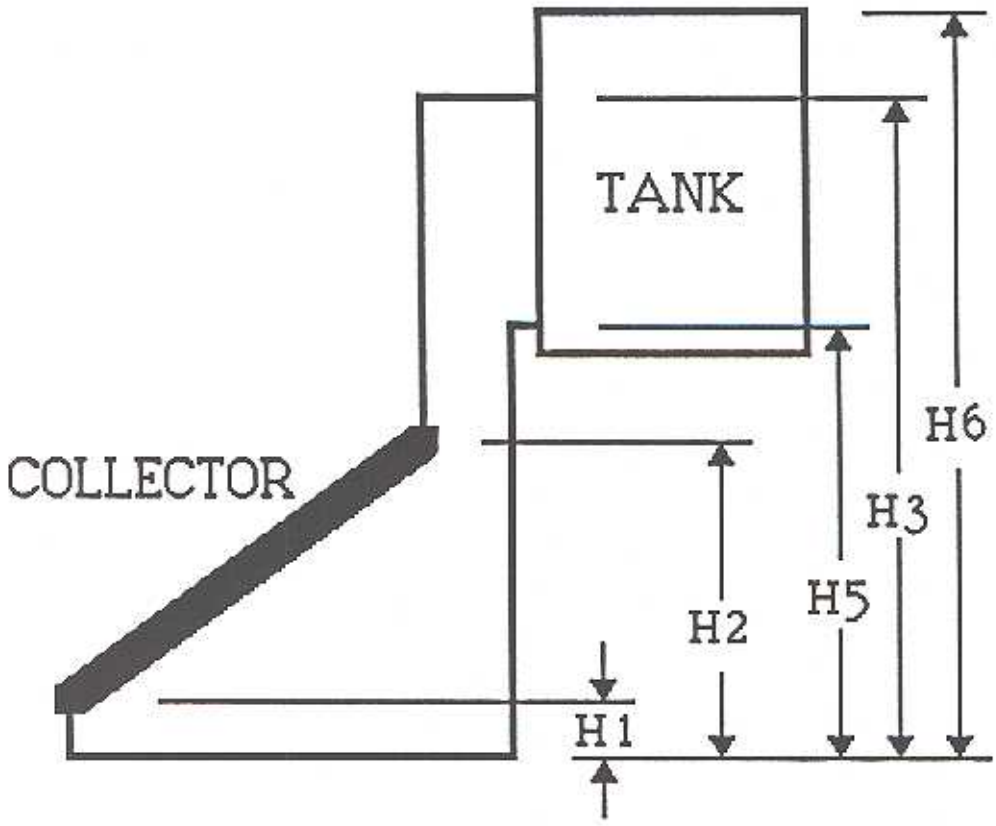

Figure 3.3 Thermosyphon system schematic showing heights needed for Equation 3.23.
From D.J. Close [12]

The Reynolds number (Re) at the estimated flow rate is calculated using a correlation for dynamic viscosity of water (μ in kg/m-sec) as a function of temperature in °C [10]:

$$\mu = \frac{0.1}{2.1482(T - 8.435 + \sqrt{8078.4 + (T - 8.435)^2}) - 120} \qquad (3.26)$$

The term $\sum ku^2/2g$ is included in the friction loss equation to account for minor losses associated with bends, tees, and other restrictions in the piping. Although the majority of the pressure drop in the flow circuit occurs across the relatively small diameter collector risers, the minor frictional losses are included to enhance the accuracy of the flow rate estimate. The pressure drop across the optional backflow prevention check valve may be included, if data for pressure drop as a function of flow rate are available from the valve manufacture. For entry from the tank to connecting pipe, $k = 0.5$. For right angle bends in the connecting pipe, the equivalent length of pipe is either increased by 30 d for laminar flow, or $k = 1$ for turbulent flow. Cross sectional changes at junctions of connecting pipes and collector headers, and headers and risers, are accounted for, depending on whether the diameter increases or decreases:

Sudden expansion:

$$K = 0.667 \left(\frac{d_1}{d_2}\right)^4 - 2.667 \left(\frac{d_1}{d_2}\right)^2 + 2 \qquad (3.27)$$

Sudden contraction:

$$K = -0.3259 \left(\frac{d_2}{d_1}\right)^4 - 0.1784 \left(\frac{d_2}{d_1}\right)^2 + 0.5 \qquad (3.28)$$

where d_1 and d_2 are the inlet and outlet pipe diameters respectively. For losses at the entry of the connecting pipe to tank, k = 1. Friction in the storage tank is neglected [10]. Developing flow in the collector risers, headers, and connecting pipes is accounted for by adjusting the friction factor as recommended by Morrison and Ranatunga [19,20]:

$$f = f + \left(1 + \frac{0.038}{\left(\frac{1}{Re \cdot d}\right)^{0.964}}\right) \qquad (3.29)$$

All the components of the friction head loss in the flow circuit at the estimated flow rate are combined and comparison made with the previously calculated thermosyphon head. If the thermosyphon head does not balance the frictional losses to within one percent, a new guess of the flow rate through the connecting pipes is made by successive substitution. The procedure is repeated with the new estimate of flow rate until convergence to within one percent is reached. Convergence is usually obtained within three iterations. The resulting single value for monthly average flow rate is that which balances the thermosyphon driving force with the frictional losses in the flow circuit. The solar fraction is calculated, assuming a fixed flow rate operating in an active system. The procedure is

carried out for each month of the year, with the previous month's "equivalent average" flow rate as the initial guess of flow rate for the new month. The fraction of the annual heating load supplied by solar energy is the sum of the monthly solar energy contributions divided by the annual load:

$$F = \frac{\sum_{i=1}^{12} F_i L_i}{\sum_{i=1}^{12} L_i} \qquad (3.30)$$

3.3 Comparison Between Design Method and TRNSYS Simulations

The design procedure outlined above was compared to detailed simulations using the TRNSYS transient simulation program. The wide range of system configurations and locations investigated are outlined in Table 3.2. Comparison between monthly solar fraction calculated by the modified f-Chart method with the iterative flow scheme for the "equivalent average" fixed flow rate, and TRNSYS simulations with 1/4 hour timesteps, for all cases listed in Table 3.2 is shown in Fig. 3.4. The monthly RMS error is 5.2%, and the monthly bias error is -1.4%. Figure 3.5 illustrates the annual solar fraction calculated by the design method, compared with annual solar fraction calculated using the detailed TRNSYS simulation. On an annual basis the RMS error is 2.6%, and the bias error is -1.5%, for all locations and system configurations studied (Table 3.2). It should be noted that for comparison purposes, values of monthly average radiation

TABLE 3.2: Range of Parameters Studied in Comparison Between the Design Method and TRNSYS Simulations

Location:	Albuquerque, NM; Madison, WI; Seattle, WA; Sterling, VA
Collector area:	1.4-5.6 m^2 (each panel 1.4 m^2)
Collector slope:	30-90°
$F_R U_L$:	3.6-8.6 W/m^2-°C
$F_R(\tau\alpha)$:	0.7-0.8
Riser diameter:	5-20 mm
# risers in each panel:	3-15
Connecting pipe diameter:	19-38 mm
Connecting pipe length:	4-12 m
# bends in connecting pipe:	4-12
Connecting pipe thermal losses:	0-11.1 W/m^2-°C
Height of storage tank above collector:	0-2 m
Storage tank size:	100-500 liters
Vertical storage tank height/diameter ratio:	1.0-2.7
Horizontal storage tank length/ diameter ratio:	2.7-5.4
Daily load draw:	150-500 liters

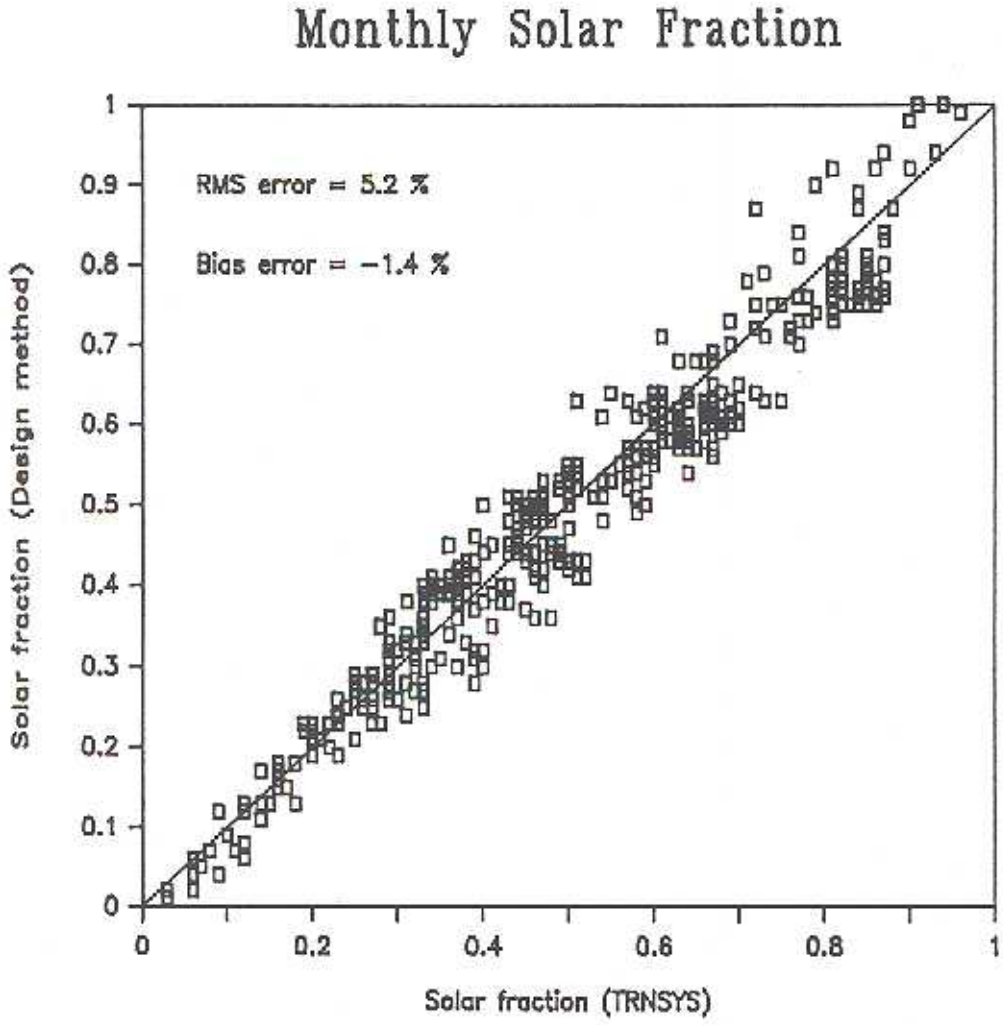

Figure 3.4 Comparison between monthly solar fraction calculated by the design method and TRNSYS simulations, for the range of systems outlined in Table 3.2

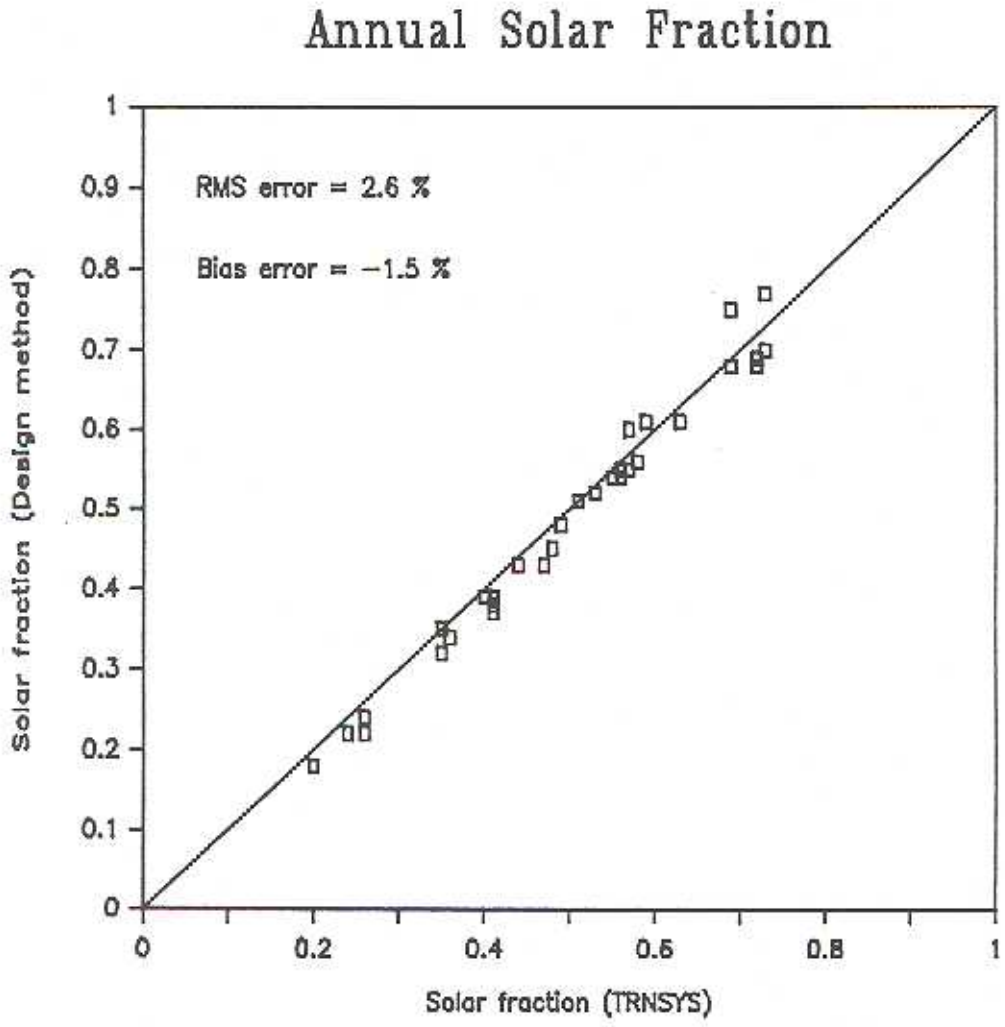

Figure 3.5 Comparison between annual solar fraction calculated by the design method and TRNSYS simulations, for the range of systems outlined in Table 3.2

incident on a tilted surface ($\bar{H}_T$) are obtained from integrating the TRNSYS hourly calculations (I_T).

The root mean square (RMS) error is a measure of the difference between the design method prediction of solar fraction and TRNSYS simulations, and is defined as:

$$\text{RMS error} = \sqrt{\sum_{i=1}^{n} (F_{design_i} - F_{TRNSYS_i})^2 / n} \qquad (3.31)$$

The RMS error places more weight on larger differences by summing the squares of the errors, and since larger errors are of more concern than smaller ones, it is a measure of the accuracy of the design method. The bias error is the average difference between the solar fraction predicted by the design method and TRNSYS simulations, and is defined as:

$$\text{Bias error} = \sum_{i=1}^{n} (F_{design_i} - F_{TRNSYS_i}) / n \qquad (3.32)$$

The bias error represents the offset of the design method relative to the simulations [32].

The design method based on the original f-Chart formulation may be easily programmed on a microcomputer, and requires only monthly average weather data, and description of the system component geometry as inputs. By the iterative scheme outlined above, the monthly and annual performance of a thermosyphon solar domestic hot water

system may be predicted, enabling design choices to be made for the sizing of the components of a system.

3.4 Example of Using the Design Method

An example of the calculation scheme used in the design method is shown for the thermosyphon system described in Table 3.3, for the month of January in Phoenix, Arizona. The monthly average meteorological data for Phoenix is found in Duffie and Beckman [1]:

$$\bar{H} = 11{,}591 \text{ kJ/m}^2\text{-day}, \quad \bar{T}_a = 10.^\circ\text{C}, \quad \bar{K}_T = 0.61$$

The monthly average solar radiation incident on the horizontal surface ($\bar{H}$) may be converted to radiation incident on the collector surface sloped at 33.4° ($\bar{H}_T$) by the method described in Duffie and Beckman, using Erbs' correlation for diffuse fraction [25]:

$$\bar{H}_T = 17{,}879 \text{ KJ/m}^2\text{-day}$$

An initial estimate of the "equivalent average" flow rate is 15 kg/hr-m^2 or 42 kg/hr for the 2.8 m^2 collector area system. The collector parameters $F_R U_L$ and $F_R(\tau\alpha)$ are corrected for the estimated flow rate at other than the ASHRAE 93-77 test conditions of 71.5 kg/hr-m^2 using Eqs. (2.3) and (2.5):

TABLE 3.3: Description of Thermosyphon System for Sample Example

Monthly average daily horizontal radiation:	11,591.0 kJ/m^2-day
Monthly average ambient temperature:	10.0°C
Monthly average clearness index:	0.61
Collector slope:	33.4°
Number of collector panels:	2.0
Collector area per panel:	1.4 m^2
Collector test parameter $F_R U_L$:	17.0 kJ/hr-m^2-°C
Collector test parameter $F_R(\tau\alpha)$:	0.80
Collector test flow rate:	71.5 kg/hr-m^2
Number of risers per panel:	10.0
Riser diameter:	0.005 m
Combined header length per panel:	1.6 m
Header diameter:	0.02 m
Tank-collector connecting pipe length:	4.0 m
Collector-tank connecting pipe length:	3.0 m
Connecting pipe diameter:	0.02 m
Number of bends in connecting pipe:	5.0
Connecting pipe heat loss coefficient:	10.0 kJ/hr-m^2-°C
Storage tank volume:	250.0 l
Storage tank height:	1.32 m
Storage tank diameter:	0.49 m
Daily load draw:	300.0 l
Mains water temperature:	12.0°C
Auxiliary set temperature:	60.0°C
Reference height (H_1):	0.0 m
Height of collector outlet above reference (H_2):	1.0 m
Height of pipe inlet to tank above reference (H_3):	2.2 m
Height of tank return to collector above reference (H_5):	1.0 m

$$F'U_L = 17.50 \text{ kJ/hr-m}^2\text{-°C}$$
$$F_RU_L = 15.28 \text{ kJ/hr-m}^2\text{-°C}$$
$$F_R(\tau\alpha) = 0.719$$

Thermal losses from the connecting pipes are accounted for by Eqs. (3.13) and (3.14):

$$F_RU_L = 16.45$$
$$F_R(\tau\alpha) = 0.711$$

Klein [32] describes how the monthly average transmittance-absorptance product ($\overline{\tau\alpha}$) may be obtained. For simplification, it is assumed that $F_R(\tau\alpha) = F_R(\overline{\tau\alpha})$. The f-Chart X and Y parameters for a fully mixed storage tank are calculated using Eqs. (3.1) and (3.2). The X parameter is corrected for a storage capacity other than 75 liters/m^2 as explained in Duffie and Beckman:

$$X_{mix} = 1.85$$
$$Y_{mix} = 0.59$$
$$F_{mix} = 0.41$$

The collector pump operating time is estimated using Evans' correlation [Eqs. (3.6)-(3.12)], and Table 3.1:

$$\beta_{max} = 62.4°$$

$$\bar{K}_T' = 0.56$$

$$A = -1.82 \times 10^{-3}$$

$$B = 9.29 \times 10^{-7}$$

$$\bar{I}_c = 12.85 \text{ W/m}^2\text{-°C}$$

$$N_p = 8.9 \text{ hr}$$

$$\bar{M}_c/M_L = 1.25$$

The stratified tank solar fraction is estimated using Copsey's correlation [Eqs. (3.4) and (3.5)]:

$$\Delta X/\Delta X_{max} = 0.60$$

$$X_{str} = 0.74$$

To find $(\overline{\tau\alpha})$ when $F_R = 1$, solve for $F_{R_{high}}/F_{R_{use}}$ at a very high flow rate (i.e., 10,000 kg/hr):

$$F_{R_{high}}/F_{R_{use}} = 1.03$$

$$(\overline{\tau\alpha}) = 0.823$$

$$Y_{max} = 0.68$$

$$F_{str} = 0.52$$

Solve for Phillips' stratification coefficient using Eqs. (3.17)-(3.19):

$$M = 4.9 \times 10^{-4}$$

$$E = 0.26$$

$$K_s = 1.16$$

Solve for the nondimensionalized average tank temperature using Eq. (3.15) or Figure 3.2:

$$\frac{\overline{T}_{tank} - T_{mains}}{\overline{T}_{set} - \overline{T}_{mains}} = 0.217$$

For $T_{mains} = 12.°C$ and $T_{set} = 60.°C$:

$$\overline{T}_{tank} = 22.4°C$$

Estimate the monthly average collector inlet temperature from Eq. (3.21):

$$\overline{T}_i = 10.6°C$$

$\overline{T}_i$ cannot be less than T_{mains}, since the connecting pipe thermal losses have already been accounted for, so $\overline{T}_i$ is set equal to $T_{mains} = 12.°C$. Estimate the monthly average collector outlet temperature using Eq. (3.22):

$$\overline{T}_o = 34.2°C$$

Solve for the specific gravity of the water at the collector inlet and outlet from Eq. (3.24):

$$S_i = 0.999208$$

$$S_o = 0.994196$$

Solve for the thermosyphon buoyancy driving force from Eq. (3.23):

$$h_T = 0.005787 \text{ m}$$

To find the frictional resistances in the flow circuit at the estimated flow rate, first estimate the viscosity from Eq. (3.26):

$$\mu = 9.48 \times 10^{-4} \text{ kg/m}^2\text{-sec}$$

Connecting Pipes:

$\dot{m}$ = 42 kg/hr

u = 0.0372 m/sec through the 0.02 m diameter pipe

Re = 783

f = 0.082

Correcting for developing flow in pipes with Eq. (3.29) gives:

$$f = 0.089$$

Including the pipe bends, and entry and exit cross sectional changes

in Eq. (3.25) yields the frictional loss in the connecting pipes:

$$h_{F_p} = 0.003231 \text{ m}$$

Risers:

Assume equal mass flow through the individual collector risers.

$\dot{m}_r = 2.1$ kg/hr

$u_r = 0.0298$ m/sec through the 0.005 m diameter risers

$Re_r = 157$

$f_r = 0.415$

$h_{F_r} = 0.006903$ m

Headers:

Approximate the flow through the entire length of the collector headers:

$$\dot{m}_h = \sum_{i=1}^{20} \dot{m}_r(i)/20 = 22.05 \text{ kg/hr}$$

$u_h = 0.0195$ m/sec through the 0.02 m diameter headers

$Re_h = 411$

$f_h = 0.170$

$h_{F_h} = 0.00054$ m

Sum the terms of the frictional head loss in the flow circuit:

$$h_F = 0.003231 \text{ m} + 0.006903 \text{ m} + 0.000540 \text{ m}$$

$$h_F = 0.01065 \text{ m}$$

Compare to the thermosyphon head from Eq. (3.23) ($h_T = 0.005787$ m):

$$\% \text{ difference} = (h_T - h_F)/h_T \times 100 = -84.5\%$$

If the frictional head loss does not match the thermosyphon head to within 1%, make a new guess of flow rate through the connecting pipes:

$$\dot{m}_{new} = \rho A \sqrt{\frac{2gh_T}{\left(\frac{fl}{d} + k\right)_p + \frac{u_r}{u}\left(\frac{fl}{d} + k\right)_r + \frac{u_h}{u}\left(\frac{fl}{d} + k\right)_h}} \qquad (3.33)$$

$$\dot{m}_{new} = 30.9 \text{ kg/hr}$$

The above procedure is repeated with the new estimate of flow rate. In the interest of saving space, only the new values of solar fraction, thermosyphon head, frictional head loss, and percentage difference are shown below:

$$F_{str} = 0.505$$

$$h_T = 0.008332 \text{ m}$$

$$h_F = 0.007852 \text{ m}$$

$$\% \text{ difference} = 5.67\%$$

Make a new guess of flow rate from Eq. (3.33):

$$\dot{m}_{new} = 31.9 \text{ kg/hr}$$

Iterate again:

$F_{str} = 0.507$

$h_T = 0.008045$ m

$h_F = 0.008084$ m

% difference = -0.49%, which is within the 1% error tolerance deemed acceptable.

The "equivalent average" flow rate for the thermosyphon system described in Table 3.3 for the month of January in Phoenix, Arizona is 31.9 kg/hr, and the monthly solar fraction is 0.51.

For February, the flow rate is initially assumed to be 31.9 kg/hr, and the same procedure is followed using the monthly average meteorological data for February:

$$\bar{H} = 15{,}595 \text{ kJ/m}^2\text{-day}, \quad \bar{T}_a = 13.^\circ\text{C}, \quad \bar{K}_T = 0.65$$

Once the monthly solar fractions have been calculated, the annual solar fraction is calculated using Eq. (3.30). For the system described in Table 3.3 in Phoenix, AZ, the annual solar fraction is 0.69.

A complete FORTRAN listing for the design method appears in Appendix B.

CHAPTER 4: FUTURE CONSIDERATIONS

4.1 Test Methods

The performance of some solar DHW systems can be approximately predicted based on the thermal characteristics of their collector array and storage tanks without a consideration of the connecting piping. The collector parameters $F_R U_L$ and $F_R(\tau\alpha)$ are determined using the ASHRAE 93-77 test method. However, many solar DHW systems, particularly natural circulation thermosyphon systems, are affected by the connecting pipes, valves, and interactions between the individual components of the system. ASHRAE Standard 95-1981 "Methods of Testing to Determine the Thermal Performance of Solar Domestic Water Heating Systems" [34] was developed to analyze the whole system as a single unit. The Standard requires that the complete system be tested indoors, using either a solar or thermal simulator. The test procedure is to measure the daily performance of the system under prescribed fixed meteorological and load conditions, until the steady state one-day performance is reached. The test is repeated until the daily system solar fraction is within three percent of the value on the previous test day. If convergence does not occur within four days, the average solar fraction for days three and four is accepted. ASHRAE specifies the method of testing the solar DHW system, but does not specify the test conditions to be used for obtaining a standard rating on which to judge the relative merit of a particular

system. This is normally done by a rating association such as the Solar Rating and Certification Corporation (SRCC).

SRCC Standard 200-82 "Test Methods and Minimum Standards for Certifying Solar Water Heating Systems" [35] defines a standard rating day to be used in conjunction with the ASHRAE Standard 95-1981 test procedure. Figure 4.1 illustrates the SRCC daily solar radiation and daily load profiles. The ambient temperature remains constant at 22°C throughout the day.

The limitation of using a selected standard rating condition is that it does not necessarily provide an accurate indication of the relative performance of a system for any weather conditions other than those specifically represented by the test. Since the ASHRAE 95-1981/SRCC 200-82 test is now commonly used for comparative rating of a variety of active and passive solar water heaters, it would be very helpful if the test results could be extended to enable prediction of the solar fraction in a variety of locations with varying day to day solar radiation and ambient temperature.

One possibility for extending the test results to predict long term performance might be through use of a catalog of "location coefficients". The solar fraction for a thermosyphon system for the ASHRAE 95-1981/SRCC 200-82 standard test day may be multiplied by a "location coefficient" to estimate the annual solar fraction for a specific location's meteorological conditions. A first step in exploring this possibility is to compare the solar fractions from the ASHRAE/SRCC test with TRNSYS annual solar fractions for a range of

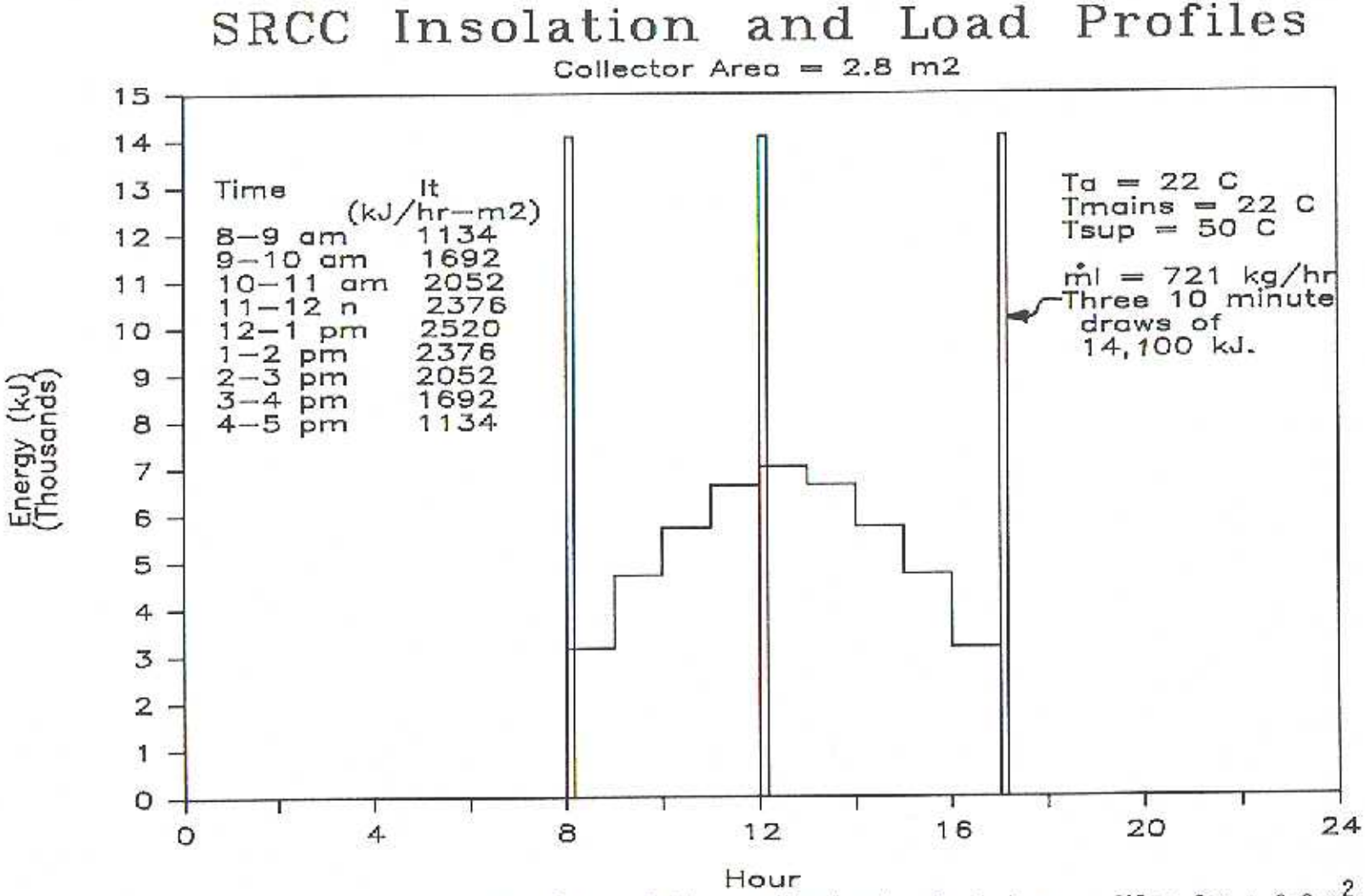

Figure 4.1 SRCC 200-82 test method solar radiation and hot water load draw profiles for a 2.8 m^2 collector area system

thermosyphon systems in a specific location. The four day test using the SRCC Standard 200-82 insolation and load profiles may also be modeled with TRNSYS so that an experimental setup is not required for the preliminary study. A complete TRNSYS deck which simulates the ASHRAE 95-1981/SRCC 200-82 test method for a thermosyphon solar DHW system appears in Appendix C. The annual solar fractions are derived from TRNSYS simulations using TMY meteorological data for Albuquerque, New Mexico, with a RAND load profile, T_{mains} = 12°C and T_{sup} = 60°C, for the range of system configurations outlined in Table 3.2. Since the SRCC standard load draw is 42,300 kJ/day, the values for solar fraction in the test results must be corrected for different loads in the annual simulations. Comparison between the test results and the annual simulations is shown in Figure 4.2. A linear least squares regression on the test results for the range of parameters shown in Table 3.3 yields a "location coefficient" of 1.30 for Albuquerque, New Mexico. This method of estimating annual solar fraction is limited in that a broad range of system configurations must be analyzed for a broad variety of locations, to yield a useful catalog of "location coefficients". Furthermore, for the many locations not as sunny as Albuquerque, the "location coefficient" will be less than one. For these locations, it would not be practical to compare large values of annual solar fraction for systems whose load is greater than the SRCC standard load with the test method solar fraction corrected for the larger load. Further work needs to be done to investigate the usefulness of such a scheme.

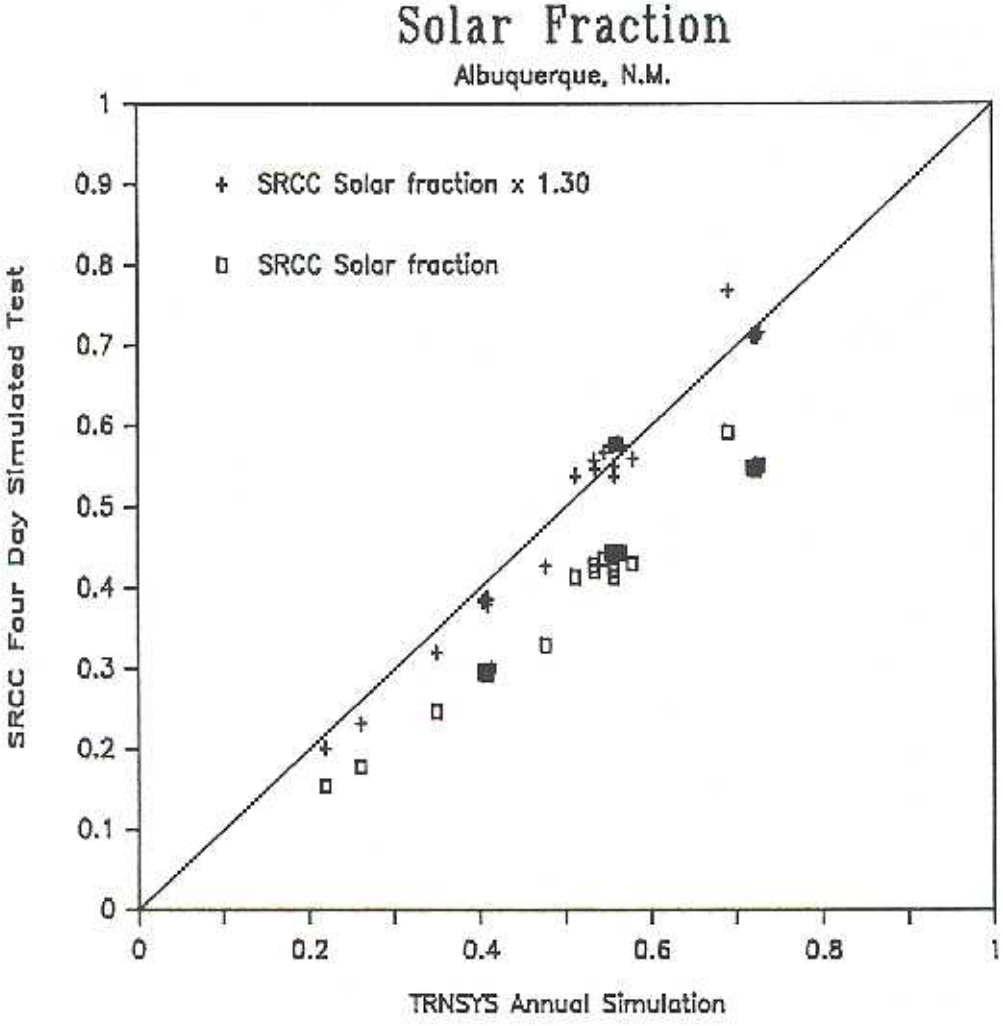

Figure 4.2 Comparison between solar fraction calculated by ASHRAE/SRCC test method, and annual TRNSYS simulations for Albuquerque, New Mexico

S.A. Klein and A.H. Fanney [36] describe a rating procedure for active solar DHW systems in which site specific weather data are combined with the ASHRAE 95-1981 test results to estimate the long term performance of an active system in a variety of locations. The testing procedure consists of two indoor tests in accordance with the ASHRAE Standard. By using the concept of solar radiation utilizability, the test results may be plotted in a manner in which the annual solar fraction of an active solar heating system may be found, independent of the standard test day conditions. It is possible that the idea of approximating the varying flow through a thermosyphon system by an "equivalent average" fixed flow rate for each month may be used to extend Klein and Fanney's rating procedure to include thermosyphon solar DHW systems. Future work should be done to explore this possibility.

4.2 Indirect Circulation

The design method described in Chapter 3 considers only direct circulation of water through the thermosyphon solar DHW system. As mentioned in Chapter 1, indirect circulation thermosyphon systems, in which an antifreeze solution circulates through the collector and transfers heat to the storage water through a heat exchanger, are currently available on the market. The penalty in collector thermal performance due to the heat exchanger in an active system may be accounted for in a manner similar to that of connecting pipe thermal losses [1]. The combination of a collector and heat exchanger per-

forms exactly like a collector alone, but with a reduced value of F_R:

$$\frac{F'_R}{F_R} = \frac{1}{1 + \left(\frac{A_c F_R U_L}{(\dot{m}c_p)_c}\right)\left(\frac{(\dot{m}c_p)_c}{\varepsilon(\dot{m}c_p)_{min}} - 1\right)} \qquad (4.1)$$

In a system where both pipe losses and a heat exchanger are present, the collector parameters should first be modified to account for pipe losses using Eqs. (3.13) and (3.14), and the modified parameters then used in Eq. (4.1) to account for the heat exchanger. This assumes that the heat exchanger is near the tank, which is usually the case. Equation (4.1) may also be used to account for the presence of a heat exchanger in a thermosyphon system. Correlations for the specific gravity and viscosity of the antifreeze solution as a function of temperature would have to be substituted for Eqs. (3.24) and (3.26), respectively. However, since no experimental data were available on long term performance of indirect circulation thermosyphon water heaters, the inclusion of Eq. (4.1) in the design method should be verified.

4.3 Conclusions

The thermal performance of a natural circulation thermosyphon solar water heating system is comparable to that of a well controlled forced circulation active solar DHW system. Thermosyphon systems have no parasitic power or maintenance requirements for a pump and

controller, and are therefore an attractive alternative for helping to meet the domestic hot water load in a variety of locations. Whereas the long term thermal performance of active systems may be estimated using the f-Chart method, there previously was no general design method available for thermosyphon systems. The purpose of this project has been to study the unique control strategy inherent in the operation of a natural circulation thermosyphon system, and to develop a design tool for predicting long term performance.

The design method which was developed is based on the original f-Chart method for active systems. The varying collector flow rate throughout the day and year in a thermosyphon system is approximated by an "equivalent average" fixed flow rate for each month in an active system. An iterative scheme has been developed for finding the flow rate which balances the thermosyphon buoyancy driving force with the frictional pressure drop in the flow circuit on a monthly average basis. The iterative scheme may be briefly outlined by the following sequence of steps:

1. The solar fraction for a stratified tank active system is evaluated for an initial estimate of flow rate using a modified form of the f-Chart method.
2. The average temperature in the thermosyphon system storage tank is calculated using a correlation between solar fraction and a non-dimensional form of the average storage temperature.

3. The temperature of the return fluid from the stratified tank to the collector is calculated using a correlation for the stratification profile in the storage tank.
4. The collector outlet fluid temperature is analytically determined, given the inlet fluid temperature and the estimated flow rate.
5. Once the collector side temperatures and the average tank temperature are known, the buoyancy force may be found.
6. The frictional losses throughout the flow circuit are calculated using conventional fluid mechanics relations for pipe flow.
7. By combining all sources of frictional resistance and comparing to the thermosyphon head, a new estimate of flow rate is found by successive substitution. The procedure is repeated with the new estimate of flow rate until the thermosyphon head balances the friction head to within one percent.

Once convergence is reached, the procedure is begun for the next month using the previous month's "equivalent average" flow rate as an initial estimate. By this iterative scheme, the monthly and annual performance of a thermosyphon solar DHW system may be predicted. A comparison between the annual solar fraction predicted by the design method and detailed TRNSYS simulations, for a wide range of thermosyphon system configurations and locations, shows an RMS error of 2.6%.

The design method can be used by a manufacturer of package thermosyphon systems or solar collectors to determine the optimal

sizes and configurations for the system components. It may also be combined with an economic analysis to allow an energy analyst, contractor, or homeowner to assess the economic as well as thermal performance of a system in a particular location. Furthermore, the benefits of changing the collector area, collector type, tank size, pipe length, diameter, and layout may easily be found, enabling the performance of a proposed or existing system to be improved.

APPENDIX A: TRNSYS DECK FOR THERMOSYPHON SOLAR DHW SYSTEMS USING TMY METEOROLOGICAL DATA

```
*THERMOSYPHON SOLAR DHW SYSTEM SIMULATION FOR ONE YEAR
*TRNSYS DECK WHICH SIMULATES THE ASHRAE STANDARD 95-1981 TEST METHOD
*WITH THE SRCC STANDARD 200-82 DAY, FOR FOUR DAY CONVERGENCE
*INCLUDES AN IN LINE AUXILIARY HEATER, AND A MIXING VALVE
*INCIDENCE ANGLE MODIFIER CONSTANT IS SET TO ZERO, TO MATCH THE
*THE ASSUMPTION THAT THE RATIO OF TAU ALPHA BAR TO TAU ALPHA
*NORMAL = 1., IN THE DESIGN METHOD

NOLIST

SIMULATION  1  8760  STEP
TOLERANCES  -0.01  -0.01
LIMITS 20 5 15
WIDTH 132

UNIT 9 TYPE 9 TMY DATA READER
PARAMETERS 13
3 1 -1 1 0 -2 1 0 -3 1 0 -1 1
(T20,F4.0,T25,F4.0,T30,F4.1)

UNIT 16 TYPE 16 SOLAR RADIATION PROCESSOR USING ERBS' CORRELATION
PARAMETERS 7
3 1 1 LAT 4871 0 -1
INPUTS 6
9,2 9,19 9,20 0,0 0,0 0,0
0.0 0.0 0.0 RHO SLOPE AZIMUTH

UNIT 14 TYPE 14 RAND LOAD PROFILE
PARAMETERS 82
0,0.0 5,0.0 5,0.125 6,0.125 6,0.391 7,0.391 7,0.625 8,0.625
8,0.703 9,0.703 9,0.549 10,0.549 10,0.391 11,0.391 11,0.297
12,0.297 12,0.422 13,0.422 13,0.242 14,0.242 14,0.203
15,0.203 15,0.156 16,0.156 16,0.297 17,0.297 17,0.549
18,0.549 18,1.0 19,1.0 19,0.786 20,0.786 20,0.549 21,0.549
21,0.422 22,0.422 22,0.391 23,0.391 23,0.156 24,0.156 24,0.0

UNIT 17 TYPE 14 DAILY USAGE
PARAMETERS 4
0,LOAD  8760,LOAD

UNIT 15 TYPE 15 INSTANTANEOUS LOAD FLOW
PARAMETERS 6
0 0 2 0 1 -4
INPUTS 3
17,1   0,0   14,1
LOAD   8.254 0.0

UNIT 45 TYPE 45 THERMOSYPHON SYSTEM
PARAMETERS 34
```

```
1  AREA  FRTAN  FRUL  71.5  BZERO  SLOPE -11 NRISER  DRISER  DHEADER
LHEADER  NODES 1.00  HCT  DIN  LIN  KI UI DOUT LOUT KO UO 1 TANK
HTANK HRET 4.19 1000.0 KTANK VERT UT 1 TMAIN
INPUTS 9
16,6 16,4 16,5 16,9  0,0  9,3  10,1   10,2  9,3
0.0  0.0  0.0  0.0   RHO  0.0  TMAIN  0.0   0.0

UNIT 10 TYPE 11 TEMPERATURE CONTROLLED FLOW DIVERTER
PARAMETERS 2
4  3
INPUTS 4
0,0    15,1  45,5  0,0
TMAIN  0.0   TSET  TSET

UNIT 11 TYPE 11  TEE PIECE
PARAMETERS 1
1
INPUTS 4
45,5   45,6  10,3   10,4
TSET   0.0   TMAIN  0.0

UNIT 6 TYPE 6   IN LINE AUXILIARY HEATER
PARAMETERS 3
12240.0 TSET 4.19
INPUTS 3
11,1  11,2   0,0
TSET  0.0    1.0

UNIT 28 TYPE 28 MONTHLY SUMMARY
PARAMETERS 30
-1 1 8760 -1 2 1 -11 -4 -12 -4 -13 -4 -14 -4 -15 -4 -16
-4 -17 -4  -18 -4 -19 -4     -17 -17 -15 3 2 -4
INPUTS 9
45,9 16,6 45,2 45,11  6,3   45,7 45,8  45,4  6,2
CHECK .10 -1,4,-6,-7
LABELS 10
DELU IT/M2 QU QU_P QAUXLN  QTLOSS  QSOL  MC  ML  SOLARF

UNIT 29 TYPE 28 MONTHLY TEMPERATURE SUMMARY
PARAMETERS 48
-1 1 8760 -1 2  -11 -2 2 -4 -12 -2 2 -4 -13 -2 2 -4 -14 -2 2 -4
-15 -2 2 -4 -16 -2 2 -4  -17 -2 2 -4     -14 -2 2  -17 -2 2  4
-1 TSET -17 -2 2 4 2 -4
INPUTS 7
45,3     45,1     45,5     45,12    11,1     6,1     10,1
LABELS 8
TTRET    TTIN     TTLOAD    TTAVE    TSOLMX   TSUPLN  TTMAIN   NONDIM

END
EOT..
```

```
CONSTANTS 35
PANEL = 1.0
KTANK = 0.0
HTANK = 1.32
HRET = 1.24
VERT = 1
UT = 3.08
MC = 50.0
LOAD = 300.0
STEP = 0.25
AREA = 1.4 * PANEL
NRISER = 10.0 * PANEL
LHEADER = 1.626 * PANEL
GTEST = 71.5
NODES = 10.0
BZERO = 0.0
KI = 1.1
KO = 4.3
UI = 0.0
UO = 0.0
LAT = 47.27
RHO = 0.2
SLOPE = LAT
AZIMUTH = 0.0
TMAIN = 12.0
TSET = 60.0
DRISER = 0.01
DHEADER = 0.0274
DIN = 0.0254
DOUT = DIN
HCT = 1.0
LIN = 4.575
LOUT = 3.355
TANK = 0.250
FRUL = 17.03
FRTAN = 0.805
EOT..
```

APPENDIX B: FORTRAN LISTING OF DESIGN METHOD FOR THERMOSYPHON SOLAR DHW SYSTEMS

```
C   THIS PROGRAM PERDICTS THE LONG TERM PERFORMANCE OF THERMOSYPHON SOLAR
C   DOMESTIC HOT WATER SYSTEMS.

C   THE VARYING COLLECTOR FLOW RATE THROUHGHOUT THE DAY AN YEAR IN A
C   THERMOSYPHON SYSTEM IS APPROXIMATED BY AN "EQUIVALENT AVERAGE" FIXED FLOW
C   RATE IN AN ACTIVE (PUMPED) SYSTEM.

C   THE "EQUIVALENT AVERAGE" FLOW RATE IS FOUND WHICH BALANCES THE BOUYANCY
C   FORCES WITH THE FRICTIONAL RESISTANCES IN THE FLOW CIRCUIT, ON A MONTHLY
C   AVERAGE BASIS.
C   AN ITERATIVE SCHEME IS USED TO FIND THIS FLOW RATE.

C   THE REQUIRED INPUTS ARE MONTHLY AVERAGE METEOROLOGICAL DATA AND DESCRIPTION
C   OF THE SYSTEM GEOMETRY.

C   OUTPUT FROM THE PROGRAM IS THE MONTHLY AND ANNUAL SOLAR FRACTION FOR THE
C   PARTICULAR SYSTEM, LOCATION, AND HOT WATER LOAD.

C   THE SOLAR FRACTION OF THE ACTIVE SYSTEM IS CALCULATED USING THE
C   F-CHART METHOD.
C   MODIFICATION FOR STORAGE TANK STRATIFICATION IS MADE USING BERNIE
C   COPSEY'S WORK.

C   A CORRELATION BETWEEN SOLAR FRACTION AND NON-DIMENSIONAL AVERAGE TANK
C   TEMPERATURE HAS BEEN DEVELOPED BASED ON TRNSYS SIMULATIONS OF A
C   VERTICAL TANK THERMOSYPHON SYSTEM WITH AN IN LINE AUXILIARY HEATER.

C   THE COLLECTOR INLET TEMP IS ESTIMATED USING THE AVERAGE TANK TEMP, AND A
C   FORM OF PHILLIPS' STRATIFICATION COEFFICIENT.


      DIMENSION  DAYS(12), BMAXAD(12), BMAX(12)
      REAL KT, KTP, L, MTEST, MUSE, MUSER, MUSEH, MHIGH, MCML
      REAL NRISEP, NRISE, LOAD
      CHARACTER*3  AMONTH(12)
      CHARACTER*4  AYEAR

      PI = 3.141593
      CONV = PI / 180.


C INPUT LATITUDE FOR PHOENIX, AZ, IN DEGREES
      DEGL = 33.43
      L = DEGL * CONV
C SET COLLECTOR SLOPE (B) AT LATITUDE
      B = L


C INPUT VALUES FOR SYSTEM CONFIGURATION AND COLLECTOR PARAMETERS
```

```
C   FROM LOGICAL UNIT 20

C NUMBER OF COLLECTOR PANELS (PANELS)
      READ(20,*) PANELS
C COLLECTOR AREA PER PANEL (AP) IN M2
      READ(20,*) AP
C INTERCEPT OF EFFICIENCY VS [TI-TA]/IT CURVE (FRULT) IN KJ/HR-M2-C
      READ(20,*) FRULT
C NEGATIVE SLOPE OF EFFICIENCY VS [TI-TA]/IT CURVE (FRTANT)
      READ(20,*) FRTANT
C MASS FLOW RATE PER UNIT COLLECTOR AREA FOR TEST CONDITIONS (GTEST)
C   IN KG/HR-M2
      GTEST = 71.5
C INCIDENCE ANGLE MODIFIER (BZ)
      BZ = -0.10
C GROUND REFLECTANCE (RHO)
      RHO = 0.2

C NUMBER OF COLLECTOR RISERS PER PANEL (NRISEP)
      READ(20,*) NRISEP
C DIAMETER OF COLLECTOR RISERS (DRISE) IN METERS
      READ(20,*) DRISE
C COMBINED HEADER LENGTH PER PANEL (HEADP) IN METERS
      READ(20,*) HEADP
C DIAMETER OF COLLECTOR HEADERS (DHEAD) IN METERS
      READ(20,*) DHEAD

C LENGTH OF INLET TO COLLECTOR CONNECTING PIPE (PIPE) IN METERS
      READ(20,*) PIPIN
C LENGTH OF OUTLET FROM COLLECTOR CONNECTING PIPE (PIPE) IN METERS
      READ(20,*) PIPOUT
C THERMAL LOSS COEFFICIENT OF CONNECTING PIPES (UPIPE) IN KJ/HR-M2-C
      READ(20,*) UPIPE
C DIAMETER OF CONNECTING PIPE (DPIPE) IN METERS
      READ(20,*) DPIPE
C NUMBER OF RIGHT ANGLE BENDS IN CONNECTING PIPE (BENDS)
      READ(20,*) BENDS

C TANK VOLUME (TANK) IN LITERS
      READ(20,*) TANK
C HEIGHT OF STORAGE TANK (HTANK) IN METERS
      READ(20,*) HTANK
C DIAMETER OF STORAGE TANK (DTANK) IN METERS
      READ(20,*) DTANK

C REFERENCE HEIGHT FOR EASE OF MEASUREMENT (H1) IN METERS
      READ(20,*) H1
C HEIGHT OF COLLECTOR OUTLET ABOVE REFERENCE (H2) IN M
      READ(20,*) H2
C HEIGHT OF CONNECTING PIPE INLET TO STORAGE TANK ABOVE REFERENCE
C   (H3) IN METERS
      READ(20,*) H3
C HEIGHT OF TANK RETURN TO COLLECTOR ABOVE REFERENCE (H5) IN M
      READ(20,*) H5
```

```
C FLUID DENSITY AT STANDARD CONDITIONS (DENS) IN KG/M3
      DENS = 1000.
C FLUID SPECIFIC HEAT AT STANDARD  (CP) IN KJ/KG-C
      CP = 4.19

C FLUID THERMAL CONDUCTIVITY AT STANDARD  (COND) IN KJ/HR-M-C
      COND = 0.6

C MAINS TEMPERATURE (TMAIN) IN C
      READ(20,*) TMAIN
C SET TEMPERATURE (TSET) IN C
      READ(20,*) TSET

C DAILY LOAD DRAW (DRAW) IN LITERS
      READ(20,*) DRAW


C CALCULATE COLLECTOR AREA (A) IN M2
      A = PANELS * AP
C CALCULATE NUMBER OF COLLECTOR RISERS (NRISE)
      NRISE = PANELS * NRISEP
C CALCULATE LENGTH OF INDIVIDUAL RISER (RISER) IN M
      RISER = (HZ-H1) / SIN(B)
C CALCULATE CROSS SECTIONAL AREA OF INDIVIDUAL RISER (CSAR) IN M2
      CSAR = PI * DRISE * DRISE / 4.
C CALCULATE TOTAL LENGTH OF HEADERS (HEAD) IN METERS
      HEADER = PANELS * HEADP
C CALCULATE CROSS SECTIONAL AREA OF HEADERS (CSAH) IN M2
      CSAH = PI * DHEAD * DHEAD / 4.
C CALCULATE COMBINED LENGTH OF CONNECTING PIPE
      PIPE = PIPIN + PIPOUT
C CALCULATE CROSS SECTIONAL AREA OF CONNECTING PIPE (CSAP) IN M2
      CSAP = PI * DPIPE * DPIPE / 4.
C CALCULATE SURFACE AREA OF INLET TO COLLECTOR CONNECTING PIPE IN M2
      SAINP = PI * DPIPE * PIPIN
C CALCULATE SURFACE AREA OF OUTLET FROM COLLECTOR CONNECTING PIPE IN M2
      SAOUTP = PI * DPIPE * PIPOUT
C CALCULATE CROSS SECTIONAL AREA OF STORAGE TANK (CSAT) IN M2
      CSAT = PI * DTANK * DTANK / 4.
C CALCULATE MASS FLOW RATE FOR TEST CONDITIONS (MTEST) IN KG/HR
      MTEST = GTEST * A
C CALCULATE HEIGHT OF TOP OF STORAGE TANK ABOVE REFERENCE (H6) IN M
      H6 = HTANK + H5

C ---------------------------------------------------------------

C NUMBER OF DAYS IN EACH MONTH
      DATA DAYS/31.,28.,31.,30.,31.,30.,31.,31.,30.,31.,30.,31./
C ARRAY OF MONTH ABBREVIATIONS (AMONTH)
      DATA AMONTH/'JAN','FEB','MAR','APR','MAY','JUN',
     &            'JUL','AUG','SEP','OCT','NOV','DEC'/
      DATA AYEAR/'YEAR'/
C SET MONTHLY OPTIMUM COLLECTOR TILT CORRECTION (BMAXAD) FOR EVANS'
C   CORRELATION IN RADIANS
      DATA BMAXAD/0.5061,0.3142,0.0524,-0.1745,-0.3840,-0.4363,
```

```
     &           -0.4189,-0.1745,-0.0349,0.1745,0.4014,0.5236/
C ---------------------------------------------------------------------
C GUESS AN INITIAL VALUE FOR COLLECTOR FLOW RATE (MUSE) IN KG/HR
C   TRY 15 KG/HR-M2
      MUSE = 15.0 * A
      KOUNT = 1
C INITIALLY SET TIN = TMAIN FOR USE IN CALCULATION OF EVANS'
C   UTILIZABILITY PUMP ON TIME.
      TIN = TMAIN
C INITIALIZE YEARLY SUMS FOR SOLAR FRACTION TO ZERO
      FMIXYN = 0.0
      FMIXYD = 0.0
      FSTRYN = 0.0
      FSTRYD = 0.0

      WRITE(6,86)
  86  FORMAT(1X,' ')
      WRITE(6,10) DEGL
  10  FORMAT(1X,'PHOENIX, AZ.: LATITUDE = ',F5.2,' DEGREES')
      WRITE(6,102) A, B/CONV
  102 FORMAT(1X,'COLLECTOR AREA =  ', F4.1, ' METERS', 5X,
     &       'COLLECTOR SLOPE =  ',F5.2,' DEGREES')
      WRITE(6,101) MUSE
  101 FORMAT(1X, ' INITIAL GUESSED VALUE FOR COLLECTOR FLOW RATE =  ',
     &       F7.2,'  KG/HR')
      WRITE(6,86)
      WRITE(6,11)
  11  FORMAT(1X,'MONTH', ' HORIZ', '  TILTED', '      XMIX', '  YMIX',
     &       '   FMIX', '    XSTR', '   YSTR', '   FSTR',
     &       '  MUSE  ^MC/ML')
      WRITE(6,12)
  12  FORMAT(1X,7X,'(KJ/M2-DAY)',T69,'(KG/HR)')

      READ(10,*)

C ---------------------------------------------------------------------

      DO 100 M=1,12,1

C INPUT MONTHLY AVERAGE METEOROLOGICAL DATA FOR A PARTICULAR LOCATION
C   (PHOENIX, AZ.) FROM LOGICAL UNIT 10

C H IS THE MONTHLY AVERAGE DAILY SOLAR RADIATION INCIDENT ON A
C   HORIZONTAL SURFACE IN KJ/M2-DAY
C TAMB IS THE MONTHLY AVERAGE AMBIENT TEMPERATURE IN C
C KT IS THE MONTHLY AVERAGE CLEARNESS INDEX

      READ(10,1) H, TAMB, KT
 1    FORMAT(T10,F5.0,T25,F2.0,T40,F4.2)

C TRANSFORM THE VALUE FOR RADIATION INCIDENT ON A HORIZONTAL SURFACE
C   TO RADIATION INCIDENT ON THE TILTED COLLECTOR SURFACE USING THE
C   SUBROUTINE "TRANSFORM"
```

```
      CALL TRANSFORM (M,L,B,H,KT,HT)

 1000 CONTINUE

C CORRECT FOR VALUES OF FRUL AND FRTAN AT FLOW RATE OTHER THAN
C ASHRAE 93-77 TEST CONDITIONS
      FPUL = -1.0*MTEST*CP/A * LOG(1.0 - (FRULT*A/MTEST/CP))
      RATNUM = MUSE*CP/A/FPUL * (1.0 - EXP(-1.0*A*FPUL/MUSE/CP))
      RATDEN = MTEST*CP/A/FPUL * (1.0 - EXP(-1.0*A*FPUL/MTEST/CP))
      RATIO = RATNUM / RATDEN
      FRTAN = FRTANT * RATIO
      FRUL = FRULT * RATIO

C CORRECT FOR THERMAL LOSSES FROM CONNECTING PIPE AS IN DUFFIE AND
C   BECKMAN, P. 357.
      TAPRIM = 1./(1. + UPIPE*SAOUTP/MUSE/CP)
      FRTAN = FRTAN * TAPRIM
      ULPRIM = (1. - UPIPE*SAINP/MUSE/CP + UPIPE*(SAINP+SAOUTP)/A/FRUL)
     &         / (1. + UPIPE*SAOUTP/MUSE/CP)
      FRUL = FRUL * ULPRIM

C CALCULATE X AND Y PARAMETERS FOR USE IN F-CHART CORRELATION
C   FOR THE SET OF UNITS PREVIOUSLY DEFINED, DELT IS THE NUMBER OF
C   HOURS IN A DAY, AND LOAD IS THE DAILY LOAD.
      TREF = 100.
      DELT = 24.
      LOAD = DRAW * CP * (TSET - TMAIN)
      XMIX = A*FRUL*(TREF - TAMB)*DELT / LOAD

C CORRECTION FOR STORAGE SIZE DIFFERENT FROM STANDARD SIZE
      STCOR = (TANK / A / 75.) ** -0.25

C CORRECTION FOR SERVICE WATER HEATING
      SWHCOR=(11.6 + 1.18*TSET + 3.86*TMAIN - 2.32*TAMB) /
     &       (100.-TAMB)
      XMIX = XMIX * STCOR * SWHCOR

C SET  RATIO OF TAU ALPHA BAR TO TAU ALPHA NORMAL = 1.
C   (INCIDENCE ANGLE MODIFIER CONSTANT IS SET = 0.)
      TAURAT = 1.0
      FRTAB = FRTAN * TAURAT
      YMIX = A*FRTAB*HT / LOAD

C CALCULATE MIXED TANK SOLAR FRACTION (FMIX) USING F-CHART CORRELATION
      FMIX = 1.029*YMIX - 0.065*XMIX - 0.245*YMIX*YMIX
     &     + 0.0018*XMIX*XMIX + 0.0215*YMIX**3

C APPLY BERNIE COPSEY CORRECTION FOR TANK STRATIFICATION

C   APPLY EVANS' CORRELATION TO ESTIMATE PUMP-ON TIME (PUMP)
      BMAX(M) = L + BMAXAD(M)
      KTP = KT*COS(0.8*(BMAX(M) - B))
      E1 = -4.86E-03 + 7.56E-03*KTP - 3.81E-03*KTP*KTP
      E2 = 5.43E-06 - 1.23E-05*KTP + 7.62E-06*KTP*KTP
      CRIT = FRUL/FRTAB*(TIN-TAMB)/3.6
```

```
C   ALLOWING CRITICAL LEVEL (CRIT) TO GO NEGATIVE
      PUMP = -HT/3.6 * (E1 + 2.*E2*CRIT)
      MCML = PUMP*MUSE / DRAW
      C1 = 1.040
      C2 = 0.726
      C3 = 1.564
      C4 = -2.760
      DELX = C1*MCML / ((C2*MCML + C3*FMIX + C4*FMIX*FMIX)**2 +1.)
      IF(DELX.GT.1.) DELX = 1.
      XSTR = XMIX * (1. - DELX)

C   DEFINE YMAX AS THE Y VALUE WHEN FR = 1.
C   IN ORDER TO DO THIS, WE MUST KNOW THE VALUE OF TAU ALPHA BAR.
C   FIND TAU ALPHA BAR BY SOLVING FOR RATIO OF FRTAN USE TO FRTAN TEST
C   AT VERY HIGH USE FLOW RATE. ESSENTIALLY THIS WILL GIVE FRTAN FOR
C   FR EQUALS 1. THEN SOLVE FOR TAU ALPHA BAR (TAUBAR) KNOWING THE
C   RATIO OF TAU ALPHA BAR TO TAU ALPHA NORMAL (TAURAT).
      MHIGH = 10000.
      RATNZ = MHIGH*CP/A/FPUL * (1.0 - EXP(-1.0*A*FPUL/MHIGH/CP))
      RATIOZ = RATNZ / RATDEN
      TANZ = FRTANT * RATIOZ
      TAUBAR = TANZ * TAURAT
      YMAX = A*TAUBAR*HT / LOAD
      YSTR = YMIX + (YMAX - YMIX) * DELX

C   CALCULATE STRATIFIED TANK SOLAR FRACTION (FSTR)
      FSTR = 1.029*YSTR - 0.065*XSTR - 0.245*YSTR*YSTR
     &      + 0.0018*XSTR*XSTR + 0.0215*YSTR**3

C   SOLAR FRACTION MUST NOT BE GREATER THAN 1.0  (OVERHEAT)
      IF(FSTR.GT.1.0)  FSTR = 1.0


C SOLVE FOR THE PHILLIPS' STRATIFICATION COEFFICIENT (PKS)
C   BASED ON TWO PARAMETERS; EFFECTIVENESS (PE) AND MIXING NUMBER (PM).

      PM = CSAT * COND / MUSE / CP / HTANK
      PE = A * FRUL / MUSE / CP
      PKS = LOG(1./(1. - PE)) / PE*(1. + PM*LOG(1./(1. - PE)))

C USING FSTR AS THE VALUE OF SOLAR FRACTION, FIND THE MEAN STORAGE TANK
C   TEMPERATURE USING A CORRELATION DEVELOPED FROM A LEAST SQUARES CURVE FIT
C   FOR A TANK (UA) VALUE = 5.27 KJ/HR-C,
      DIMNON = 0.117*FSTR + 0.356*FSTR*FSTR + 0.424*(FSTR**3)
      TTANK = TMAIN + DIMNON*(TSET - TMAIN)

C SOLVE FOR THE TEMPERATURE OF RETURN FLUID FROM THE TANK TO THE
C   COLLECTOR (TIN) USING PHILLIPS' STRATIFICATION COEFFICIENT

C NEED TO USE THE NUMBER OF HOURS OF PUMP ON TIME TO INTEGRATE (IT) TO (HT)
      TIN = PKS*TTANK + (1. - PKS)*(FRTAB/FRUL*HT/PUMP + TAMB)

C SET THE COLLECTOR INLET TEMPERATURE TO MAINS TEMPERATURE IF PHILLIPS'
C   GIVES A VALUE FOR (TIN) LESS THAN MAINS.
      IF(TIN.LT.TMAIN) TIN = TMAIN
```

```
C SET THE COLLECTOR INLET TEMPERATURE TO TANK TEMPERATURE IF PHILLIPS'
C   GIVES A VALUE FOR (TIN) GREATER THAN TTANK.
      IF(TIN.GT.TTANK) TIN = TTANK

C SOLVE FOR THE COLLECTOR OUTLET TEMPERATURE (TOUT) WHEN THE ABSORBED
C   SOLAR RADIATION IS APPROXIMATED AS HT*TAUBAR.
      TOUT=TIN + A/MUSE/CP/PUMP*(HT*FRTAB - FRUL*PUMP*(TIN - TAMB))

C USING CORRELATIONS FOR SPECIFIC GRAVITY AND VISCOSITY OF WATER FROM
C TRNSYS TYPE45, FIND THE THERMOSYPHON HEAD (THHEAD) USING THE EQUATION
C FROM CLOSE, SOLAR ENERGY 6,  P. 33.
      SG1 = 1.00026 - 3.906E-05*TIN - 4.05E-06*TIN*TIN
      SG2 = 1.00026 - 3.906E-05*TOUT - 4.05E-06*TOUT*TOUT
      SGTANK = 1.00026 - 3.906E-05*TTANK - 4.05E-06*TTANK*TTANK

C GRAVITATIONAL CONSTANT (GRAV) IN M/SEC2
      GRAV = 9.81

      THHEAD = 0.5*(SG1 - SG2) * (2*(H3-H1) - (H2-H1) -
     &                                  (H3-H5)*(H3-H5)/(H6-H5))

C CALCULATE THE DYNAMIC VISCOSITY AT THE AVERAGE TANK TEMPERATURE (VIS)
C IN KG/M-SEC.
      VIS = 0.1/(2.1482*(TTANK - 8.435 +
     &                SQRT(8078.4 + (TTANK - 8.435)**2))-120.)


C ---------------   CONNECTING PIPE  ----------------------

C MASS FLOW RATE OF WATER THROUGH CONNECTING PIPE (FLOW) IN M/SEC.
      FLOW = MUSE / (SGTANK*DENS*CSAP*3600.)
C CALCULATE REYNOLDS' NUMBER IN CONNECTING PIPE (REP)
      REP = SGTANK*DENS*FLOW*DPIPE / VIS
C FRICTION FACTOR (FRICTP) IN PIPE DEPENDS ON WHETHER FLOW IS LAMINAR
C (REYNOLDS' NUMBER < 2000.) OR TURBULENT (REYNOLDS' NUMBER > 2000.).
C ACCOUNT FOR BENDS IN CONNECTING PIPE.
      IF(REP.LT.2000.) THEN
         FRICTP = 64./REP
         EQPIPE = PIPE + BENDS*30.*DPIPE
         TBENDS = 0.0
      END IF

      IF(REP.GE.2000.)
         FRICTP = 0.032
         EQPIPE = PIPE
         TBENDS = BENDS
      END IF

C DEVELOPING FLOW IN CONNECTING PIPES
      FRICTP = FRICTP *(1. + 0.038/(PIPE/(REP*DPIPE))**0.964)

C ENTRY FROM TANK TO CONNECTING PIPE
      TBENDS = TBENDS + 0.5
C CROSS SECTION CHANGE AT JUNCTION OF CONNECTING PIPES AND HEADER
```

```
      IF(DPIPE.LT.DHEAD) TBENDS = TBENDS + 0.667*(DPIPE/DHEAD)**4
     &                           - 2.667*(DPIPE/DHEAD)**2 + 2.0
      IF(DPIPE.GT.DHEAD) TBENDS = TBENDS - 0.3259*(DHEAD/DPIPE)**4
     &                           - 0.1784*(DHEAD/DPIPE)**2 + 0.5
C EXIT FROM CONNECTING PIPE TO TANK
      TBENDS = TBENDS + 1.0

      FRHDP = FRICTP*EQPIPE*FLOW*FLOW / (2.*GRAV*DPIPE)
     &        + TBENDS*FLOW*FLOW/(2.*GRAV)

C ----------------   CONNECTING PIPE  ----------------------

C ----------------------  RISERS  -------------------------

C ASSUME EQUAL MASS FLOW THROUGH COLLECTOR RISERS (MUSER) IN KG/HR
      MUSER = MUSE / NRISE
C MASS FLOW RATE OF WATER THROUGH RISER (FLOWR) IN M/SEC.
      FLOWR = MUSER / (SGTANK*DENS*CSAR*3600.)
      RATRP = FLOWR / FLOW
C CALCULATE REYNOLDS' NUMBER IN RISERS (RER)
      RER = SGTANK*DENS*FLOWR*DRISE / VIS
C FRICTION FACTOR (FRICTR) IN RISER DEPENDS ON WHETHER FLOW IS LAMINAR
C (REYNOLDS' NUMBER < 2000.) OR TURBULENT (REYNOLDS' NUMBER > 2000.).
      IF(RER.LT.2000.)  FRICTR = 64./RER
      IF(RER.GE.2000.)  FRICTR = 0.032

C DEVELOPING FLOW IN RISERS
      FRICTR = FRICTR *(1. + 0.038/(RISER/(RER*DRISE))**0.964)

C CROSS SECTION CHANGE AT JUNCTION OF RISER AND HEADER
      IF(DRISE.LT.DHEAD) CROSSR = 0.667*(DRISE/DHEAD)**4
     &                           - 2.667*(DRISE/DHEAD)**2 + 2.0
      IF(DRISE.GT.DHEAD) CROSSR = - 0.3259*(DHEAD/DRISE)**4
     &                           - 0.1784*(DHEAD/DRISE)**2 + 0.5

      FRHDR = FRICTR*RISER*FLOWR*FLOWR / (2.*GRAV*DRISE)
     &        + CROSSR*FLOWR*FLOWR/(2.*GRAV)

C ----------------------  RISERS  -------------------------

C ----------------------  HEADERS  ------------------------

C APPROXIMATE MASS FLOW RATE THROUGH ENTIRE LENGTH OF HEADER (MUSEH) IN KG/HR
      MUSEH = 0.0
      DO 500 I=1,INT(NRISE),1
         MUSEH = MUSEH + MUSER*REAL(I)/NRISE
  500 CONTINUE
C MASS FLOW RATE OF WATER THROUGH HEADER (FLOWH) IN M/SEC.
      FLOWH = MUSEH / (SGTANK*DENS*CSAH*3600.)
      RATHP = FLOWH / FLOW
C CALCULATE REYNOLDS' NUMBER IN HEADER (REH)
      REH = SGTANK*DENS*FLOWH*DHEAD / VIS
C FRICTION FACTOR (FRICTH) IN HEADER DEPENDS ON WHETHER FLOW IS LAMINAR
C (REYNOLDS' NUMBER < 2000.) OR TURBULENT (REYNOLDS' NUMBER > 2000.).
      IF(REH.LT.2000.)  FRICTH = 64./REH
```

```
      IF(REH.GE.2000.)  FRICTH = 0.032

C DEVELOPING FLOW IN HEADER
      FRICTH = FRICTH *(1. + 0.038/(HEADER/(REH*DHEAD))**0.964)

C CROSS SECTION CHANGE AT JUNCTION OF HEADER AND RISER
      IF(DHEAD.LT.DRISE) CROSSH = 0.667*(DHEAD/DRISE)**4
     &                           - 2.667*(DHEAD/DRISE)**2 + 2.0
      IF(DHEAD.GT.DRISE) CROSSH = - 0.3259*(DRISE/DHEAD)**4
     &                           - 0.1784*(DRISE/DHEAD)**2 + 0.5

C CROSS SECTION CHANGE AT JUNCTION OF HEADER AND CONNECTING PIPE
      IF(DHEAD.LT.DPIPE) CROSSH = CROSSH + 0.667*(DHEAD/DPIPE)**4
     &                           - 2.667*(DHEAD/DPIPE)**2 + 2.0
      IF(DHEAD.GT.DPIPE) CROSSH = CROSSH - 0.3259*(DPIPE/DHEAD)**4
     &                           - 0.1784*(DPIPE/DHEAD)**2 + 0.5

      FRHDH = FRICTH*HEADER*FLOWH*FLOWH / (2.*GRAV*DHEAD)
     &         + CROSSH*FLOWH*FLOWH/(2.*GRAV)

C ---------------------  HEADERS  ------------------------


C  COMBINE FRICTIONAL LOSSES IN CONNECTING PIPES, RISERS AND HEADERS
      FRHEAD = FRHDP + FRHDR + FRHDH


C ** ITERATION TO FIND FLOW RATE WHICH BALANCES THERMOSYPHON HEAD
C    WITH FRICTIONAL LOSSES  TO ONE PERCENT **
      IF(KOUNT.GT.10) THEN
            WRITE(6,998) AMONTH(M)
            GO TO 999
        END IF
  998       FORMAT(1X,'**** YOUVE ITERATED MORE THAN TEN TIMES FOR ',
     &A3, '**** ')

      DIFFER = (THHEAD - FRHEAD)/THHEAD * 100.

      IF(ABS(DIFFER).LT.1.) GO TO 999

C  FOR THERMOSYPHON HEAD LESS THAN ZERO (REVERSE FLOW IN WINTER), SET
C    TO ZERO (I.E., INCLUDING A CHECK VALVE).

      IF(THHEAD.LT.0.0) THEN
         WRITE(6,88) AMONTH(M)
   88    FORMAT(1X,'*WARNING* REVERSE FLOW OCCURS IN '.A3.'. FLOW RATE
     &RE-INITIALIZED TO 15 KG/HR-M2')
         GO TO 999
      END IF

      MUSE = SGTANK*DENS*CSAP*3600.*SQRT(2.*GRAV*THHEAD /
     &   ((FRICTP*EQPIPE/DPIPE + TBENDS) + (RATRP*RATRP)*(FRICTR*RISER
     &    /DRISE + CROSSR) + (RATHP*RATHP)*(FRICTH*HEADER/DHEAD +
     &    CROSSH)))
```

```
      KOUNT = KOUNT + 1

      GO TO 1000

  999 CONTINUE

C   PRINT THE RESULTS
      WRITE(6,21) AMONTH(M), H, HT, XMIX, YMIX, FMIX, XSTR, YSTR,
     &            FSTR, MUSE, MCML
   21 FORMAT(1X, A3, 2F9.1, 8F7.2)

C   SUM FOR ANNUAL SOLAR FRACTIONS FOR MIXED AND STRATIFIED TANKS
      FMIXYN = FMIXYN + FMIX*LOAD*DAYS(M)
      FMIXYD = FMIXYD + LOAD*DAYS(M)
      FSTRYN = FSTRYN + FSTR*LOAD*DAYS(M)
      FSTRYD = FSTRYD + LOAD*DAYS(M)

C   RESET THE VALUE OF THE COUNTER (KOUNT) FOR THE NEW MONTH
      KOUNT = 1

C  SET FLOW RATE INITIALLY TO 15 KG/HR-M2 FOR NEXT MONTH AFTER REVERSE
C  FLOW OCCURS
      IF(THHEAD.LT.0.0)  MUSE = 15.0 * A

  100 CONTINUE

      FMIXYR = FMIXYN / FMIXYD
      FSTRYR = FSTRYN / FSTRYD
      WRITE(6,22) AYEAR, FMIXYR, FSTRYR
   22 FORMAT(1X,A4,T37,F7.2,T58,F7.2)

      STOP
      END

      SUBROUTINE TRANSFORM (M,L,B,H,KT,HT)

C TRANSFORM RADIATION INCIDENT INCIDENT ON A HORIZONTAL SURFACE TO
C   RADIATION INCIDENT ON THE COLLECTOR SLOPED AT AN ANGLE B WITH
C   RESPECT TO THE HORIZONTAL USING ERBS' CORRELATION FOR DIFFUSE
C   FRACTION

      DIMENSION  D(12)
      REAL L, KT

C DECLINATION ANGLE (D) FOR MEAN DAY IN EACH MONTH IN RADIANS
      DATA D/-0.3648, -0.2269, -0.0419, 0.1641, 0.3281, 0.4032,
     &       0.3700, 0.2356, 0.0384, -0.1676, -0.3299, -0.4014/

C SET GROUND REFLECTANCE RHO
      RHO = 0.2

C CALCULATE SUNSET HOUR ANGLE FOR HORIZONTAL SURFACE (WS)
C   FOR MEAN DAY OF MONTH, IN RADIANS
      WS = ACOS(-1.0*TAN(L) * TAN(D(M)))
C CALCULATE SUNSET HOUR ANGLE FOR TILTED SURFACE (WSP)
```

```
C   FOR MEAN DAY OF MONTH, IN RADIANS
      WSP = MIN(ACOS(-1.0*TAN(L) * TAN(D(M))),
     &             ACOS(-1.0*TAN(L-B) * TAN(D(M))))

C CALCULATE RATIO OF BEAM RADIATIN ON A TILTED SURFACE TO THAT ON
C   A HORIZONTAL SURFACE (RB). FOR SOUTH FACING SURFACES IN THE
C   NORTHERN HEMISPHERE
      RBNUM = COS(L-B)*COS(D(M))*SIN(WSP) + WSP*SIN(L-B)
     &     *SIN(D(M))
      RBDEN = COS(L)*COS(D(M))*SIN(WS) + WS*SIN(L)*SIN(D(M))
      RB = RBNUM / RBDEN

C CHECK IF KT IS IN RANGE OF ERBS' CORRELATION  0.3 < KT < 0.8
      IF(KT.LT.0.3.OR.KT.GT.0.8) WRITE(6,99) KT
   99 FORMAT(1X,'**** WARNING **** , KT = ',F4.2,' ,WHICH IS OUT OF
     &       RANGE OF ERBS CORRELATION')
C USING ERBS' CORRELATION, CALCULATE DIFFUSE FRACTION (HDRATIO)
      HDRAT = 1.317 - 3.023*KT + 3.372*KT*KT
     &             - 1.760*KT**3
      HD = H * HDRAT

C   CALCULATE RADIATION INCIDENT ON TILTED SURFACE (HT) AS SUM OF
C   BEAM, DIFFUSE, AND GROUND REFLECTED RADIATION
      HT = H*(1.0-HDRAT)*RB + HD*((1.0+COS(B))/2.0)
     &       + H*RHO*((1.0-COS(B))/2.0)
      RETURN
      END
EOT..
```

```
        2.0         # OF COLLECTOR PANELS
        1.4         COLLECTOR AREA PER PANEL [M²]
        17.00       FRUL [KJ/HR-M²C]
        0.80        FRTAN
        10.0        # RISERS/PANEL
        0.005       RISER DIAMETER [M]
        1.6         COMBINED HEADER LENGTH PER PANEL [M]
        0.02        HEADER DIAMETER [M]
        4.0         COLLECTOR INLET PIPE LENGTH [M]
        3.0         COLLECTOR OUTLET PIPE LENGTH [M]
        10.0        PIPE THERMAL LOSSES [KJ/HR-M²C]
        0.02        PIPE DIAMETER [M]
        5.0         # BENDS IN PIPE
        250.0       TANK VOLUME [L]
        1.32        HEIGHT OF STORAGE TANK [M]
        0.49        DIAMETER OF STORAGE TANK [M]
        0.0         REFERENCE HEIGHT [M] (H ONE)
        1.0         COLLECTOR OUTLET ABOVE REF [M] (H TWO)
        2.2         PIPE INLET TO TANK ABOVE REF [M] (H THREE)
        1.0         TANK RETURN TO COLL ABOVE REF [M] (H FIVE)
        12.0        MAINS WATER TEMPERATURE [C]
        60.0        AUXILIARY SET TEMPERATURE [C]
        300.0       DAILY LOAD DRAW [L]
EOT..
```

MONTH	H (KJ/M2-DAY)	TAMB (C)	KT
JAN	11591.	10.	0.61
FEB	15595.	13.	0.65
MAR	20588.	15.	0.69
APR	26725.	19.	0.75
MAY	30375.	24.	0.77
JUN	31087.	29.	0.76
JUL	28219.	32.	0.70
AUG	26019.	31.	0.70
SEP	22873.	28.	0.71
OCT	17892.	22.	0.70
NOV	13057.	15.	0.65
DEC	10577.	11.	0.60

EOT..

PHOENIX, AZ.: LATITUDE = 33.43 DEGREES
COLLECTOR AREA = 2.8 METERS COLLECTOR SLOPE = 33.43 DEGREES
INITIAL GUESSED VALUE FOR COLLECTOR FLOW RATE = 42.00 KG/HR

MONTH	HORIZ (KJ/MZ-DAY)	TILTED	XMIX	YMIX	FMIX	XSTR	YSTR	FSTR	MUSE (KG/HR)	^MC/ML
JAN	11591.0	17879.0	1.77	0.56	0.40	0.78	0.63	0.51	31.85	0.95
FEB	15595.0	21353.8	1.69	0.69	0.50	0.61	0.77	0.62	36.33	1.16
MAR	20588.0	24332.0	1.65	0.81	0.58	0.45	0.90	0.71	43.29	1.40
APR	26725.0	27087.4	1.52	0.92	0.66	0.26	1.01	0.80	51.04	1.68
MAY	30375.0	27178.2	1.32	0.92	0.67	0.20	1.02	0.80	51.63	1.76
JUN	31087.0	26303.6	1.10	0.89	0.67	0.18	0.99	0.78	50.32	1.76
JUL	28219.0	24607.4	0.97	0.82	0.63	0.21	0.91	0.74	45.93	1.69
AUG	26019.0	24933.1	1.01	0.84	0.64	0.21	0.93	0.75	47.24	1.67
SEP	22873.0	25436.1	1.14	0.86	0.64	0.22	0.95	0.76	48.17	1.66
OCT	17892.0	23636.1	1.37	0.78	0.58	0.37	0.87	0.70	43.68	1.42
NOV	13057.0	19788.9	1.60	0.64	0.46	0.63	0.71	0.57	35.43	1.09
DEC	10577.0	16902.1	1.72	0.53	0.37	0.79	0.59	0.48	31.11	0.90
YEAR					0.57			0.69		

EOT..

APPENDIX C: TRNSYS DECK FOR SIMULATING THE ASHRAE 95-1981 / SRCC 200-82 TEST METHOD FOR THERMOSYPHON SOLAR DHW SYSTEMS

```
*THERMOSYPHON SOLAR DHW SYSTEM
*TRNSYS DECK WHICH SIMULATES THE ASHRAE STANDARD 95-1981 TEST METHOD
*WITH THE SRCC STANDARD 200-82 DAY, FOR FOUR DAY CONVERGENCE
*INCLUDES AN IN LINE AUXILIARY HEATER, AND A MIXING VALVE

CONSTANTS 33
PANEL = 4.0
KTANK = 0.0
HTANK = 1.32
HRET = 1.24
VERT = 1
UT = 3.08
AREA = 1.4 * PANEL
NRISER = 10.0 * PANEL
LHEADER = 1.626 * PANEL
STEP = 0.167
GTEST = 71.5
NODES = 10.0
BZERO = 0.0
KI = 1.1
KO = 4.3
UI = 0.0
UO = 0.0
RHO = 0.2
SLOPE = 45.0
AZIMUTH = 0.0
TAMB = 22.0
TMAIN = 22.0
TSET = 50.0
DRISER = 0.00493
DHEADER = 0.0274
DIN = 0.0254
DOUT = DIN
HCT = 1.0
LIN = 4.575
LOUT = 3.355
TANK = 0.250
FRUL = 17.03
FRTAN = 0.805

NOLIST

SIMULATION  17  113  STEP
TOLERANCES  -0.01  -0.01
LIMITS 20 5 15
WIDTH 132

UNIT 46 TYPE 14 SRCC SOLAR IRRADIANCE PROFILE (KJ/HR-M2)
```

```
PARAMETERS 44
0,0. 8,0. 8,1134. 9,1134. 9,1692. 10,1692. 10,2052. 11,2052. 11,2376.
12,2376. 12,2520. 13,2520. 13,2376. 14,2376. 14,2052. 15,2052. 15,1692.
16,1692. 16,1134. 17,1134. 17,0. 24,0.

UNIT 47 TYPE 14 SRCC INCIDENCE ANGLE
PARAMETERS 44
0,90. 8,90. 8,60. 9,60. 9,45. 10,45. 10,30. 11,30. 11,15.
12,15. 12,0. 13,0. 13,15. 14,15. 14,30. 15,30. 15,45.
16,45. 16,60. 17,60. 17,90. 24,90.

UNIT 48 TYPE 14 SRCC LOAD FORCING FUNCTION
*DRAW OF 14,100 KJ AT RATE OF 0.2 KG/SEC.
*EQUIVALENT TO TSET=50 C, TMAIN=22 C, AND 120 KG IN 10 MINUTES.
PARAMETERS 28
0,0. 8,0. 8,721. 8.167,721. 8.167,0. 12,0. 12,721. 12.167,721. 12.167,0.
17,0. 17,721. 17.167,721. 17.167,0. 24,0.

UNIT 45 TYPE 45 THERMOSYPHON SYSTEM
PARAMETERS 34
1  AREA  FRTAN  FRUL  71.5  BZERO  SLOPE -11 NRISER  DRISER  DHEADER
LHEADER  NODES 1.00  HCT  DIN  LIN  KI UI DOUT LOUT KO UO 1 TANK
HTANK HRET 4.19 1000.0 KTANK VERT UT 1 TMAIN
INPUTS 9
46,1 0,0  0,0  47,1  0,0   0,0   10,1   10,2  0,0
0.0  0.0  0.0  90.0   RHO  TAMB  TMAIN  0.0   TAMB

UNIT 10 TYPE 11 TEMPERATURE CONTROLLED FLOW DIVERTER
PARAMETERS 2
4  3
INPUTS 4
0,0    48,1  45,5  0,0
TMAIN  0.0   TSET  TSET

UNIT 11 TYPE 11  TEE PIECE
PARAMETERS 1
1
INPUTS 4
45,5   45,6  10,3   10,4
TSET   0.0   TMAIN  0.0

UNIT 6 TYPE 6   IN LINE AUXILIARY HEATER
PARAMETERS 3
84600.0 TSET 4.19
INPUTS 3
11,1  11,2   0,0
TSET  0.0    1.0

UNIT 28 TYPE 28 SUMMARY
PARAMETERS 30
24 17 113 -1 2 1 -11 -4 -12 -4 -13 -4 -14 -4 -15 -4 -16
-4 -17 -4  -18 -4 -19 -4      -17 -17 -15 3 2 -4
INPUTS 9
45,9  46,1 45,2 45,11  6,3   45,7 45,8  45,4  6,2
CHECK .10 -1,4,-6,-7
```

```
LABELS 10
DELU IT/M2 QU QU_P QAUXLN  QTLOSS  QSOL  MC  ML  SOLARF

UNIT 29 TYPE 28 TEMPERATURE SUMMARY
PARAMETERS 48
24 17 113 -1 2  -11 -2 2 -4 -12 -2 2 -4 -13 -2 2 -4 -14 -2 2 -4
-15 -2 2 -4 -16 -2 2 -4  -17 -2 2 -4     -14 -2 2  -17 -2 2  4
-1 TSET -17 -2 2 4 2 -4
INPUTS 7
45,3     45,1     45,5      45,12    11,1     6,1      10,1
LABELS 8
TTRET    TTIN     TTLOAD    TTAVE    TSOLMX   TSUPLN   TTMAIN   NONDIM

END
EOT..
```

REFERENCES

[1] J.A. Duffie and W.A. Beckman, Solar Engineering of Thermal Processes, John Wiley and Sons, Inc., New York, (1980).

[2] B. Norton and S.D. Probert, "Recent Advances in Natural-Circulation, Solar-Energy Water Heater Designs," Applied Energy 15, pp. 15-42, (1983).

[3] W.S. Fleming & Associates, Solar Domestic and Service Hot Water Manual, American Society of Heating, Refrigerating and Air-Conditioning Engineers, Inc., Atlanta, (1983).

[4] A.H. Fanney and S.A. Klein, "Performance of Solar Domestic Hot Water Systems at the National Bureau of Standards," Journal of Solar Energy Engineering 105, pp. 311-321, (1983).

[5] A.H. Fanney and S.T. Liu, "Comparing Experimental and Computer Predicted Performance for Solar Hot Water Systems," ASHRAE Journal, May (1980).

[6] A.H. Fanney and S.A. Klein, "Thermal Performance Comparisons for Solar Hot Water Systems Subjected to Various Collector Array Flow Rates," Proceedings ISES Conference, Montreal, to be published (1985).

[7] M.D. Wuestling et al., "Promising Control Alternatives for Solar Water Heating Systems," Journal of Solar Energy Engineering 107, pp. 215-221, August (1985).

[8] A.B. Copsey, "A Modification of the f-Chart Method for Solar Domestic Hot Water Systems with Stratified Storage," M.S. Thesis, University of Wisconsin-Madison, (1984).

[9] G.L. Morrison and J.E. Braun, "System Modeling and Operation Characteristics of Thermosyphon Solar Water Heaters," Solar Energy 34, pp. 389-405, (1985).

[10] S.A. Klein et al., TRNSYS 12.1 User's Manual, University of Wisconsin, Solar Energy Laboratory, (1983).

[11] J.J. Mutch, "Residential Water Heating: Fuel Conservation, Economics and Public Policy," Rand Corporation R-1498-NSF, May (1974).

[12] D.J. Close, "The Performance of Solar Water Heaters with Natural Circulation," Solar Energy 6, pp. 33-40, (1962).

[13] C.L. Gupta and H.P. Garg, "System Design in Solar Water Heaters with Natural Circulation," Solar Energy 12, pp. 163-182, (1968).

[14] K.S. Ong, "A Finite Difference Method to Evaluate the Thermal Performance of a Solar Water Heater," Solar Energy 16, pp. 137-147, (1974).

[15] K.S. Ong, "An Improved Computer Program for the Thermal Performance of a Solar Water Heater," Solar Energy 18, pp. 183-191, (1976).

[16] J.A. Baughn and D.A. Dougherty, "Experimental Investigation and Computer Modeling of a Solar Natural Circulation System," AS-ISES Annual Meeting, (1977)

[17] M.S. Sodha and G.N. Tiwari, "Analysis of Natural Circulation Solar Water Heating Systems," Energy Con. and Mgmt. 21, pp. 283-288, (1981).

[18] Y. Zvirin et al., "The Natural Circulation Solar Heater Models with Linear and Nonlinear Temperature Distributions," International Journal of Heat and Mass Transfer 20, pp. 997-999 (1977).

[19] G.L. Morrison and D.B.J. Ranatunga, "Transient Response of Thermosyphon Solar Collectors," Solar Energy 24, pp. 55-61, (1980).

[20] G.L. Morrison and D.B.J. Ranatunga, "Thermosyphon Circulation in Solar Collectors," Solar Energy 24, pp. 191-198, (1980).

[21] B.J. Huang, "Similarity Theory of Solar Water Heater with Natural Circulation," Solar Energy 25, pp. 105-116, (1980).

[22] A. Mertol et al., "Detailed Loop Model (DLM) Analysis of Liquid Solar Thermosyphons with Heat Exchangers," Solar Energy 27, pp. 367-386, (1981).

[23] G.L. Morrison and C.M. Sapsford, "Long Term performance of Thermosyphon Solar Water Heaters," Solar Energy 30, pp. 341-350, (1983).

[24] I.J. Hall et al., "Generation of a Typical Meteorological Year," Proceedings of 1978 Annual Meeting, American Section of the ISES, 2., p. 669 (1978).

[25] D.G. Erbs, "Methods for Estimating the Diffuse Fraction of Hourly, Daily, and Monthly Average Global Solar Radiation," M.S. Thesis, University of Wisconsin-Madison, (1980).

[26] M.J. Brandemuehl and W.A. Beckman, "Transmission of Diffuse Radiation Through CPC and Flat Plate Collector Glazings," Solar Energy 24, pp. 511-513, (1980).

[27] M.D. Wuestling, "Investigation of Promising Control Alternatives for Solar Water Heating Systems," M.S. Thesis, University of Wisconsin-Madison (1983).

[28] S.A. Klein et al., "A Design Procedure for Solar Heating Systems," Solar Energy 18, pp. 113-127, (1976).

[29] J.C. Mitchell et al., "Calculation of Monthly Average Collector Operating Time and Parasitic Energy Requirements," Solar Energy 26, pp. 555-558, (1981).

[30] D.L. Evans et al., "A New Look at Long Term Collector Performance and Utilizability," Solar Energy 28, pp. 13-23, (1982).

[31] W.F. Phillips and R.N. Dave, "Effects of Stratification on the Performance of Liquid-Based Solar Heating Systems," Solar Energy 29, pp. 111-120, (1982).

[32] D.G. Erbs, "Models and Applications for Weather Statistics Related to Building Heating and Cooling Loads, Ph.D. Thesis, University of Wisconsin-Madison, (1984).

[33] S.A. Klein, "Calculation of the Monthly Average Transmittance-Absorptance Product," Solar Energy 23, pp. 547-551, (1979).

[34] American Society of Heating, Refrigerating, and Air-Conditioning Engineers, ASHRAE Standard 95-1981, Methods of Testing to Determine the Thermal Performance of Solar Domestic Hot Water Heating Systems, (1981).

[35] Solar Rating and Certification Corporation, SRCC Standard 200-82, Test Methods and Minimum Standards for Certifying Solar Water Heating Systems, (1985).

[36] S.A. Klein and A.H. Fanney, "A Rating Procedure for Solar Domestic Water Heating Systems," Transactions of the ASME 105, (1983).